RSC Advances

PAPER

View Article Online
View Journal | View Issue

Cite this: *RSC Adv.*, 2025, **15**, 47565

Design, synthesis, and biological evaluation of novel 3-oxo-2,3-dihydropyridazine derivatives as interleukin-2-inducible T-cell kinase (ITK) inhibitors

Sudhakar Tangallapalli,[ab] Rambabu Gundla,*[a] Kalyani Paidikondala,[a] Soňa Gurská,[cd] Naveen Kumar Rampeesa,[b] Sreenivasa Reddy Anugu,[b] Petr Džubák,[cd] Marián Hajdúch,[cd] Viswanath Das *[cd] and Naresh Kumar Katari *[e]

This study reports the design, synthesis, and biological evaluation of a novel series of 3-oxo-2,3-dihydropyridazine derivatives, representing a previously unexplored scaffold for selective inhibition of interleukin-2-inducible T-cell kinase (ITK), with potential application in T-cell leukemia treatment. Cytotoxicity was assessed across a panel of ITK-expressing leukemia cell lines (Jurkat, CCRF-CEM), Bruton's tyrosine kinase (BTK)-positive lines (Ramos, K562), ITK/BTK-null cancer cells, and non-cancerous fibroblasts to determine therapeutic selectivity. Compound **9** emerged as the lead candidate, showing selective ITK inhibition in biochemical kinase assays (half-maximal inhibitory concentration, IC_{50} = 0.87 μM) with no measurable BTK inhibition, moderate cytotoxicity in Jurkat cells (cellular IC_{50} = 37.61 μM), and did not show measurable cytotoxicity in fibroblasts (IC_{50} > 50 μM). In contrast, **22** exhibited greater potency in both kinase [IC_{50} (ITK) = 0.19 μM] and cytotoxicity assay [IC_{50} (Jurkat) = 11.17 μM], but showed partial BTK inhibition, indicating reduced selectivity. Structure–activity relationship analysis indicated that the 3,5-difluorophenyl and furan-2-ylmethyl groups in **22** contributed to potency, while the 3-fluorophenyl group in **9** was associated with improved selectivity. Importantly, western blot analysis confirmed that **9** reduced phosphorylation of ITK (Tyr551/Tyr511) and downstream extracellular signal-regulated kinase 1/2 (ERK1/2) (Thr202/Tyr204) in phytohemagglutinin-stimulated Jurkat cells, supporting on-target inhibition of ITK signaling. These results position **9** as a selective ITK inhibitor with a favorable therapeutic index, establishing a foundation for further optimization and preclinical development.

Received 2nd September 2025
Accepted 24th November 2025

DOI: 10.1039/d5ra06565h

rsc.li/rsc-advances

1. Introduction

Interleukin-2-inducible T-cell kinase (ITK) plays a central role in T-cell receptor (TCR) signaling and immune cell communication. As a non-receptor tyrosine kinase, ITK acts as a critical mediator that translates TCR signal strength into specific gene expression profiles, thereby shaping T-cell fate and function.[1] It is expressed in various immune cells, including mast cells, natural killer (NK) cells, and T lymphocytes.[2] ITK regulates early signaling events, including calcium mobilization, activation of phospholipase C gamma (PLCγ), and cytoskeletal rearrangements.[3] While ITK contributes to IL-2 production, it is more strongly associated with Th2-type responses by promoting the secretion of IL-4, IL-5, and IL-13.[4] Given its multifaceted role in immune regulation, ITK has been implicated in a range of autoimmune, allergic, and inflammatory conditions, positioning it as a valuable therapeutic target.[5] The novelty of this work lies in introducing the 3-oxo-2,3-dihydropyridazine scaffold as a previously unexplored chemotype for selective ITK inhibition, supported by integrated biochemical, cellular, and computational validation.

Recent evidence also highlights ITK's involvement in cancer. Elevated ITK expression has been observed in several tumor types and is linked to poor clinical outcomes. For instance, ITK expression is significantly higher in tumor tissues than in normal tissues and correlates with worse prognosis in head and neck squamous cell carcinoma.[6] In malignant T-cell lines, both genetic knockdown and pharmacological inhibition of ITK suppressed migration, invasion, and proliferation.[7] The selective ITK inhibitor BMS-509744 induced pro-apoptotic signaling and G_2/M cell cycle arrest.[7] Furthermore, ITK inhibition

[a]*Department of Chemistry, School of Science, GITAM University, Hyderabad 502102, Telangana, India. E-mail: rgundla@gitam.edu; Tel: +91-9849869933*

[b]*Aragen Life Sciences Ltd, Medicinal Chemistry Laboratory Division, Hyderabad 500076, India*

[c]*Institute of Molecular and Translational Medicine, Czech Advanced Technologies and Research Institute, Palacký University Olomouc, Křížkovského 511/8, Olomouc 77900, Czech Republic*

[d]*Institute of Molecular and Translational Medicine, Faculty of Medicine and Dentistry, Palacký University and University Hospital Olomouc, Hněvotínská 1333/5, Olomouc 77900, Czech Republic. E-mail: viswanath.das@upol.cz; Tel: +420 585 632 111*

[e]*School of Chemistry & Physics, College of Agriculture, Engineering & Science, Westville Campus, University of KwaZulu-Natal, P Bag X 54001, Durban 4000, South Africa. E-mail: KatariN@ukzn.ac.za; Tel: +14093652520*

potentiated the effects of chemotherapeutic agents like doxorubicin and vincristine, suggesting its utility in combination regimens.[8] These findings reinforce ITK as a promising target for therapeutic intervention in T-cell malignancies.

Heterocyclic compounds with a pyridazine scaffold have long been recognized as versatile pharmacophores in medicinal chemistry. The pyridazine ring is found in several clinically approved drugs such as pipofezine, cadralazine, hydralazine, and minaprine.[9] Structurally, pyridazine is a six-membered aromatic ring containing two adjacent nitrogen atoms (positions 1 and 2), offering multiple substitution sites that can modulate physicochemical and biological properties.[10] Among its derivatives, 3-oxo-2,3-dihydropyridazine analogs have shown promise due to their diverse pharmacological profiles, including anti-inflammatory, anticancer, and immunomodulatory activities.[11] The scaffold's synthetic flexibility makes it an attractive platform for designing inhibitors that can selectively engage kinase targets, such as ITK.[12]

In this study, we report the design, synthesis, and biological evaluation of a focused library of 3-oxo-2,3-dihydropyridazine derivatives as potential ITK inhibitors. A structure-guided design strategy was employed, incorporating molecular docking to identify favorable interactions with ITK. Synthesized compounds were evaluated for cytotoxicity across a panel of cancer and non-cancer cell lines that differed in ITK/BTK (Bruton's tyrosine kinase) expression. Selected compounds were prioritized based on their therapeutic index (TI) and docking affinity. This integrated approach aims to identify structurally tractable ITK inhibitors with potential utility in T-cell malignancies.

2. Results

2.1 Synthesis and structural design of 3-oxo-2,3-dihydropyridazine derivatives

To efficiently optimize the biological potency, selectivity, and physicochemical properties of 3-oxo-2,3-dihydropyridazine derivatives, a concise and modular synthetic strategy was developed. This approach enabled systematic structural diversification at key positions of the scaffold to explore structure–activity relationships (SAR). Specifically, modifications were targeted at the R^2 position on the azetidine moiety and the C-6 position of the pyridazinone core through (hetero)aryl substitution.

The synthesis was initiated from the core scaffold, 4-bromo-6-chloropyridazin-3(2*H*)-one. Substitution at the left-hand side (LHS) was achieved through nucleophilic displacement using various azetidin-3-yl compounds to incorporate the azetidine ring. This was followed by Suzuki–Miyaura coupling at the C-6 position, employing a variety of boronic acids to install structurally diverse aryl and heteroaryl substituents. The modular nature of this synthetic route facilitated the rapid generation of analogues for pharmacological profiling. The overall design was adapted from previously reported ITK inhibitors based on 3-aminopyridin-2-one derivatives (Fig. 1), where structural modifications were introduced at the R^1 position *via* heteroaryl groups and at R^2 with amine functionalities to enhance bioactivity and selectivity.[13]

The developed synthetic route proved to be robust and versatile, affording a range of 3-oxo-2,3-dihydropyridazine derivatives in good to excellent yields across various substitution patterns. The azetidine substitution reactions proceeded efficiently under mild conditions, while the Suzuki couplings displayed broad functional group tolerance, enabling incorporation of both electron-rich and electron-deficient substituents at the C-6 position. All final compounds were purified to high purity and structurally characterized using ^{1}H NMR, ^{13}C NMR, and mass spectrometry.

Preliminary biological evaluations (where applicable) indicated that certain substituents enhanced the desired cytotoxic activity, laying the foundation for subsequent SAR exploration. Five distinct molecular scaffolds were synthesized using this strategy, with each designed to probe the contribution of specific substitutions to ITK/BTK selectivity and cytotoxic potency.

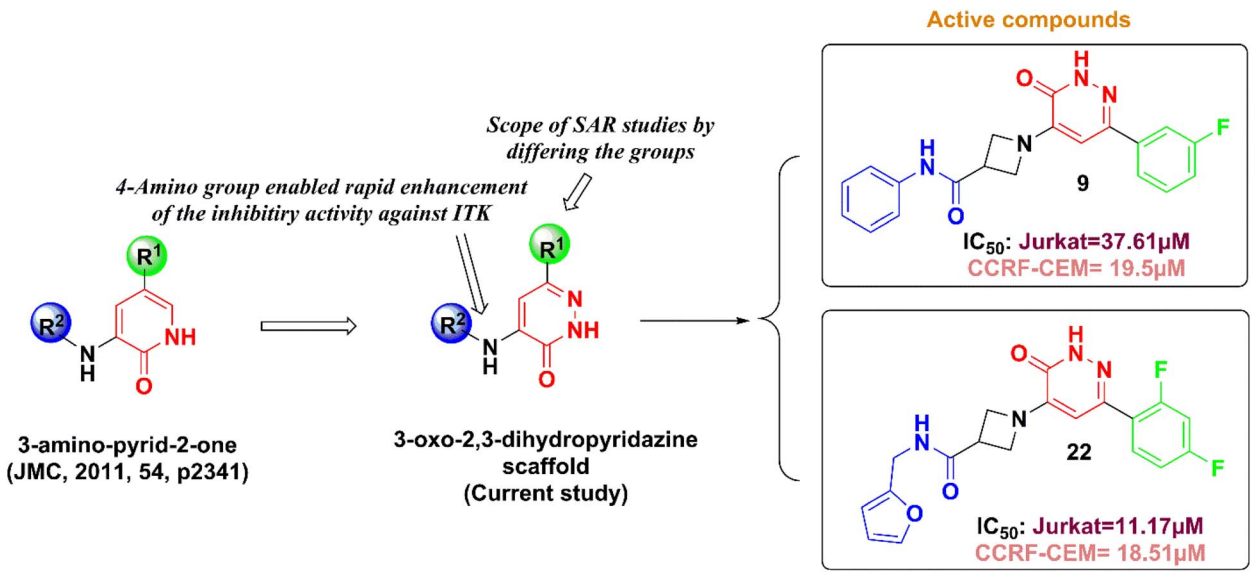

Fig. 1 Rational design for 3-oxo-2,3-dihydropyridazine derivatives.

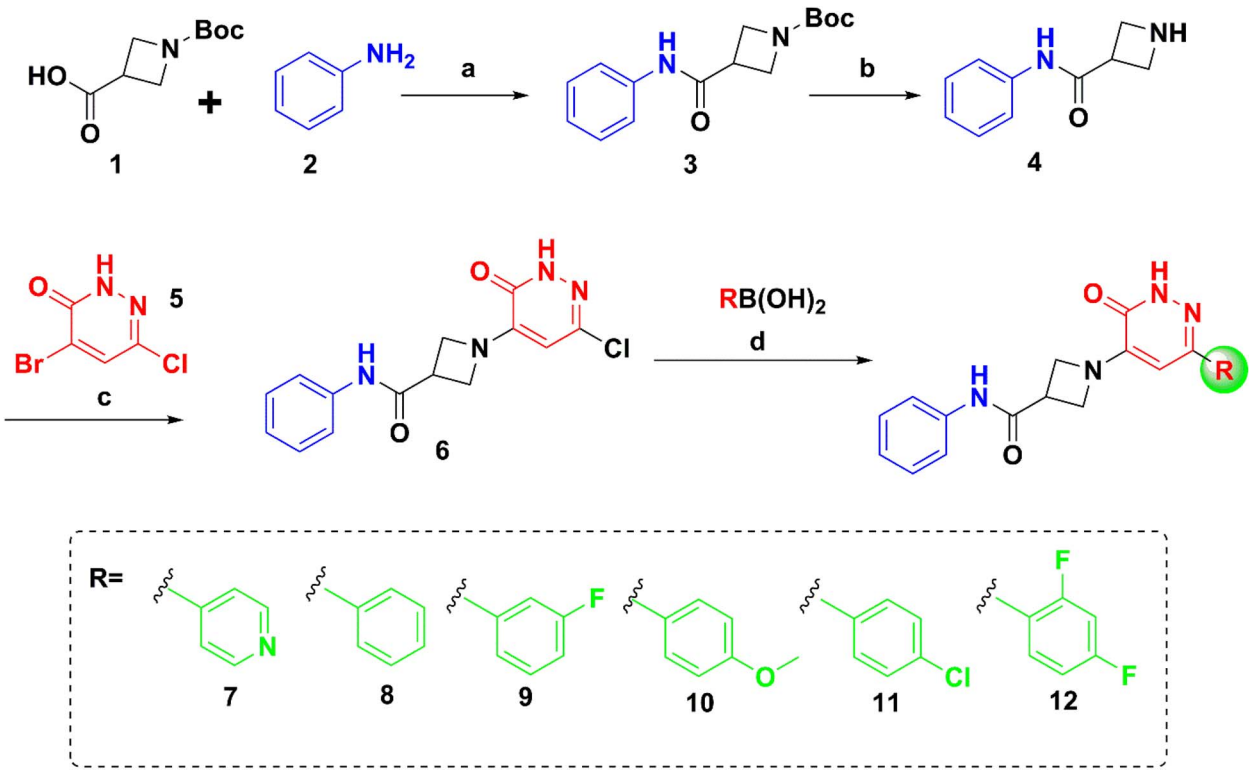

Scheme 1 Synthesis of compounds **7–12**. Reagents and conditions: (a) HATU, DIPEA, DMF, RT; (b) TFA, CH_2Cl_2, RT; (c) DIPEA, DMF, RT; (d) boronic acid, 2 N Na_2CO_3, $Pd(dppf)Cl_2 \cdot CH_2Cl_2$, 1,4-dioxane, 100 °C.

Table 1 Cytotoxicity of 3-oxo-2,3-dihydropyridazine derivatives (compounds **7–12**) in human cancer and non-cancer cell lines. IC_{50} values in μM (data are presented as the mean of ≥6 replicates). Therapeutic index (TI) was calculated using fibroblast cell lines: TI* = BJ/Jurkat; TI‡ = MRC-5/Jurkat. n. d. = not determined

	ITK/BTK null				BTK positive		ITK positive		Non-cancer			
Cmpd	A549	HCT116	HCT116-p53	U2OS	RAMOS	K562	Jurkat	CCRF-CEM	BJ	MRC-5	TI*	TI‡
7	>50	>50	>50	>50	>50	>50	>50	>50	>50	>50	n. d.	n. d.
8	>50	>50	>50	>50	>50	>50	>50	>50	>50	>50	n. d.	n. d.
9	>50	>50	>50	>50	9.58	>50	37.61	19.5	>50	43.16	>1.33	1.55
10	>50	>50	>50	>50	10.95	>50	40.33	20.78	>50	>50	>1.24	>1.24
11	32.02	38.9	37.93	26.95	10.44	>50	33.21	23.04	33.97	26	1.02	0.78
12	36.34	37.07	32.77	16.2	16.82	31.76	33.93	18.02	28.88	16.56	0.85	0.49

2.2 Synthesis and cytotoxic evaluation of scaffold 1 derivatives (compounds 7–12)

Compounds **7–12** were synthesized as the first set of analogues using the general route outlined in Scheme 1. The intermediate compound **3** was obtained by amide coupling between 1-(*tert*-butoxycarbonyl)azetidine-3-carboxylic acid **1** and aniline **2**, followed by Boc-deprotection to afford compound **4**. This was subjected to nucleophilic substitution with 4-bromo-6-chloropyridazin-3(2*H*)-one (**5**) to yield intermediate **6**, which underwent Suzuki–Miyaura coupling with a range of boronic acids to afford the final derivatives **7–12**.

The cytotoxic effects of compounds **7–12** were evaluated using the MTS assay across a panel of human cancer and non-cancer cell lines representing different ITK expression statuses (Table 1). This panel included ITK-expressing T-cell lines (Jurkat, CCRF-CEM), BTK-expressing B-cell lines (RAMOS, K562), ITK-null solid tumor lines (A549, HCT116, HCT116-p53, U2OS), and non-cancerous human fibroblast cell lines (BJ, MRC-5). TI was calculated using IC_{50} values in fibroblast cell lines (BJ or MRC-5) divided by the IC_{50} in Jurkat cells, given that Jurkat cells express high levels of ITK and are considered the more biologically relevant model for assessing ITK-targeted cytotoxicity.

Among the tested compounds, **9** exhibited the most promising profile within this scaffold. It showed moderate cytotoxicity in CCRF-CEM (IC_{50} = 19.5 μM) and lower activity in Jurkat cells (IC_{50} = 37.61 μM), with acceptable TI values (>1.33 for BJ and 1.55 for MRC-5), suggesting some degree of selectivity toward ITK-expressing cells. In contrast, **7** and **8** were inactive (IC_{50} > 50 μM

across all tested lines), indicating a lack of cytotoxic potential. Compound **10** exhibited moderate activity in ITK-positive cells (IC_{50} = 40.33 μM in Jurkat; 20.78 μM in CCRF-CEM) with minimal off-target effects, although its selectivity was lower than compound **9**. Compounds **11** and **12** exhibited IC_{50} values ranging from 18 to 37 μM across multiple cancer lines but also displayed moderate toxicity in BJ and MRC-5 cells, resulting in TI values close to or below 1, indicating reduced selectivity relative to Jurkat cells. These findings suggest that within Scaffold 1, compound **9** presents the most balanced profile of moderate ITK-targeted activity and limited toxicity in non-cancerous cells, meriting further consideration. These results clearly identify compound **9** as the most selective ITK-targeted molecule within scaffold 1, combining moderate cytotoxicity in ITK-expressing cells with minimal off-target toxicity.

2.3 Synthesis and cytotoxic evaluation of scaffold 2 derivatives (compounds 17–23)

Scaffold 2 derivatives (compounds **17–23**) were synthesized as shown in Scheme 2. The synthesis began with an amide coupling between 1-(*tert*-butoxycarbonyl)azetidine-3-carboxylic acid (**1**) and furan-2-ylmethanamine (**13**), yielding **14**. This was followed by Boc deprotection to obtain **15**. This intermediate was then reacted *via* nucleophilic substitution with 4-bromo-6-chloropyridazin-3(2*H*)-one (**5**) to produce **16**. The final Suzuki–Miyaura coupling with various boronic acids resulted in the generation of products **17–23**.

Within this scaffold, **23** exhibited the strongest cytotoxicity against ITK-expressing cells, with IC_{50} values of 5.15 μM (Jurkat) and 5.12 μM (CCRF-CEM), and exceptionally high TI values (>9.71 for both fibroblast lines) (Table 2). However, this compound also demonstrated low IC_{50} values in non-ITK cancer cells (*e.g.*, 8.83 μM in HCT116 and 5.53 μM in RAMOS), indicating broad cytotoxicity and poor selectivity, which led to its deprioritization despite its high potency. As such, despite its potency, **23** was deprioritized for further development. In contrast, **22** demonstrated a more favorable balance of moderate cytotoxicity in Jurkat (11.17 μM), CCRF-CEM (18.51 μM), Ramos (22.34 μM), and K562 (21.40 μM) cells, while maintaining IC_{50} > 36 μM in all non-ITK/BTK cancer lines and >50 μM in fibroblast cells. TI values exceeded 4.48, suggesting selective toxicity in ITK-expressing cells. This profile supported the prioritization of compound **22** for downstream validation. Compound **22** emerged as the lead of scaffold **2**, showing an optimal balance of potency and therapeutic selectivity across the tested panel.

Compounds **18–21** exhibited modest cytotoxicity in Jurkat cells (IC_{50} = 19.20–30.50 μM) and lower activity in CCRF-CEM or BTK-expressing lines, while compound **17** was completely inactive (IC_{50} > 50 μM in all tested cells). Overall, compound **22** emerged as the strongest candidate from scaffold 2 based on its combined potency, TI, and selectivity. For reference, we have previously reported the cytotoxicity profiles of ibrutinib in ITK- and BTK-positive cell lines using the same screening setup[14,15] and these data serve as internal benchmarks in our ongoing assay workflow.

2.4 Synthesis and cytotoxic evaluation of scaffold 3 derivatives (compounds 28–29)

Scaffold 3 was constructed through the synthetic sequence outlined in Scheme 3. Starting with the amide coupling between

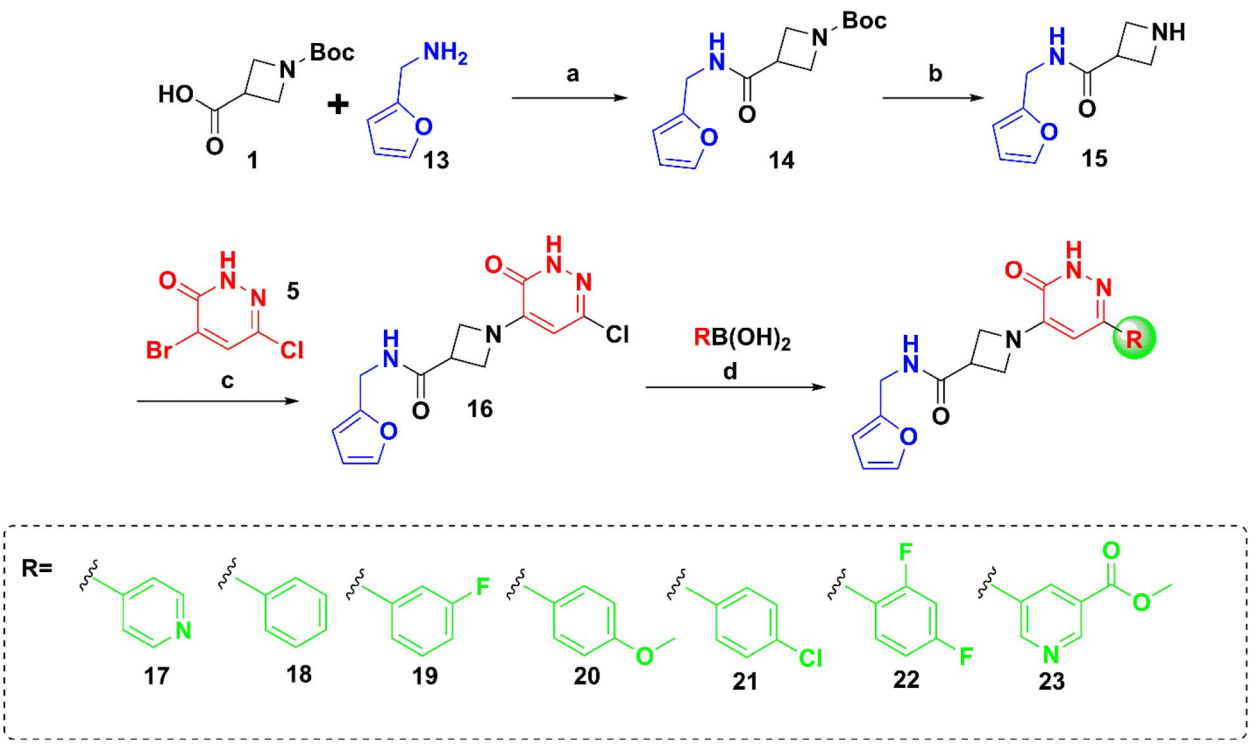

Scheme 2 Synthesis of compounds **17–23**. Reagents and conditions: (a) HATU, DIPEA, DMF, RT; (b) TFA, CH_2Cl_2, RT; (c) DIPEA, DMF, RT; (d) boronic acid, 2 N Na_2CO_3, $Pd(dppf)Cl_2 \cdot CH_2Cl_2$, 1,4-dioxane, 100 °C.

Table 2 Cytotoxicity of scaffold 2 derivatives (compounds **17–23**) in human cancer and non-cancer cell lines. IC_{50} values in μM (data are presented as the mean of ≥6 replicates). Therapeutic index (TI) was calculated using fibroblast cell lines: TI* = BJ/Jurkat; TI‡ = MRC-5/Jurkat

	ITK/BTK null				BTK positive		ITK positive		Non-cancer			
Cmpd	A549	HCT116	HCT116-p53	U2OS	RAMOS	K562	Jurkat	CCRF-CEM	BJ	MRC-5	TI*	TI‡
17	>50	>50	>50	>50	>50	>50	>50	>50	>50	>50	n. d.	n. d.
18	>50	>50	>50	>50	41.19	30.43	19.24	30.2	>50	>50	>2.60	>2.60
19	>50	>50	>50	>50	16.29	>50	25.07	>50	>50	>50	>1.99	>1.99
20	>50	>50	>50	>50	19.71	38.69	24.34	>50	>50	>50	>2.00	>2.00
21	>50	>50	>50	>50	37.46	>50	30.47	>50	>50	>50	>1.64	>1.64
22	>50	40.27	41.25	36.23	22.34	21.4	11.17	18.51	>50	>50	>4.48	>4.48
23	42.11	8.83	12.67	16.87	5.53	7.4	5.15	5.12	>50	>50	>9.71	>9.71

1-(*tert*-butoxycarbonyl)azetidine-3-carboxylic acid (**1**) and 1-phenylpiperazine (**24**), the reaction yielded **25**, which underwent Boc-deprotection to afford **26**. This intermediate was then subjected to nucleophilic substitution with 4-bromo-6-chloropyridazin-3(2*H*)-one (**5**) to form **27**, followed by Suzuki coupling with appropriate boronic acids to yield final products **28** and **29**.

Biological evaluation revealed that both compounds were inactive across all tested cancer cell lines and non-cancerous fibroblast models, with IC_{50} values >50 μM (Table 3). This lack of activity presumably suggests poor cellular permeability, metabolic instability, or insufficient binding affinity despite favorable docking scores obtained for **29**.

2.5 Synthesis and cytotoxic evaluation of scaffold 4 derivatives (compounds 34–39)

Scaffold 4 was synthesized *via* the route shown in Scheme 4. Initial amide coupling between 1-(*tert*-butoxycarbonyl) azetidine-3-carboxylic acid (**1**) and 2,2,2-trifluoroethan-1-amine (**30**) yielded **31**, which, upon Boc-deprotection, afforded **32**. This intermediate was then reacted with 4-bromo-6-chloropyridazin-3(2*H*)-one (**5**) to give **33**, followed by Suzuki coupling with a variety of boronic acids to generate final derivatives **34–39**.

Cytotoxicity profiling (Table 4) revealed that compounds **34–37** were completely inactive across all tested cell lines (IC_{50} > 50 μM), suggesting poor cellular activity. Compounds **38** and **39** showed only weak to marginal activity. Compound **38** exhibited low cytotoxicity against Jurkat (IC_{50} = 44.9 μM) and CCRF-CEM (IC_{50} = 29.95 μM), whereas **39** was mildly active only in CCRF-CEM (IC_{50} = 26.75 μM). No significant cytotoxicity was detected in non-cancerous BJ or MRC-5 fibroblasts for either compound.

2.6 Synthesis and cytotoxic evaluation of scaffold 5 derivatives (compounds 46 and 52)

2.6.1. Synthesis of scaffold 5a – compound 46. The synthesis of **46** is outlined in Scheme 5. The key intermediate **43** was obtained through the reaction of *tert*-butyl 3-oxoazetidine-1-carboxylate (**40**) with *p*-toluenesulfonylhydrazine, forming a hydrazone intermediate, which was subsequently reacted with isonicotinaldehyde (**42**) and a base to yield *tert*-butyl 3-isonicotinoylazetidine-1-carboxylate (**43**). Boc-deprotection of

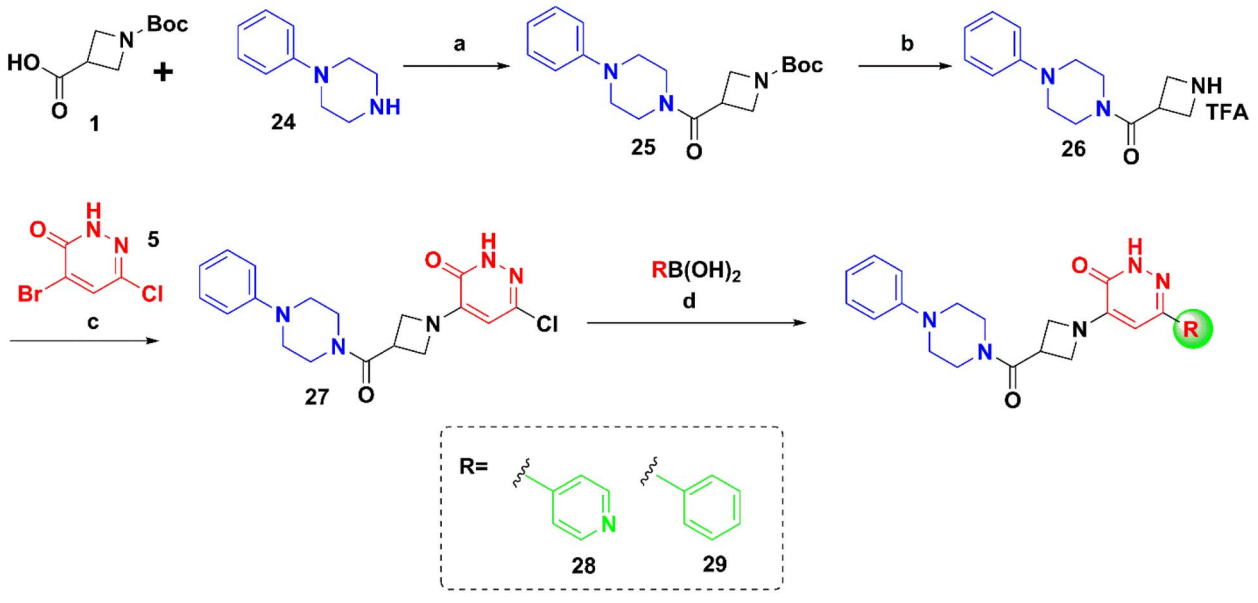

Scheme 3 Synthesis of compounds **28** and **29**. Reagents and conditions: (a) HATU, DIPEA, DMF, RT; (b) TFA, CH_2Cl_2, RT; (c) DIPEA, DMF, RT; (d) boronic acid, 2 N Na_2CO_3, $Pd(dppf)Cl_2 \cdot CH_2Cl_2$, 1,4-dioxane, 100 °C.

Table 3 Cytotoxicity of scaffold 3 derivatives (compounds **28** and **29**) in cancer and non-cancer cell lines. IC_{50} values in μM (data are presented as the mean of ≥6 replicates). Therapeutic index (TI) was calculated using fibroblast cell lines: TI* = BJ/Jurkat; TI‡ = MRC-5/Jurkat

	ITK/BTK null				BTK positive		ITK positive		Non-cancer			
Cmpd	A549	HCT116	HCT116-p53	U2OS	RAMOS	K562	Jurkat	CCRF-CEM	BJ	MRC-5	TI*	TI‡
28	>50	>50	>50	>50	>50	>50	>50	>50	>50	>50	n. d.	n. d.
29	>50	>50	>50	>50	>50	>50	>50	>50	>50	>50	n. d.	n. d.

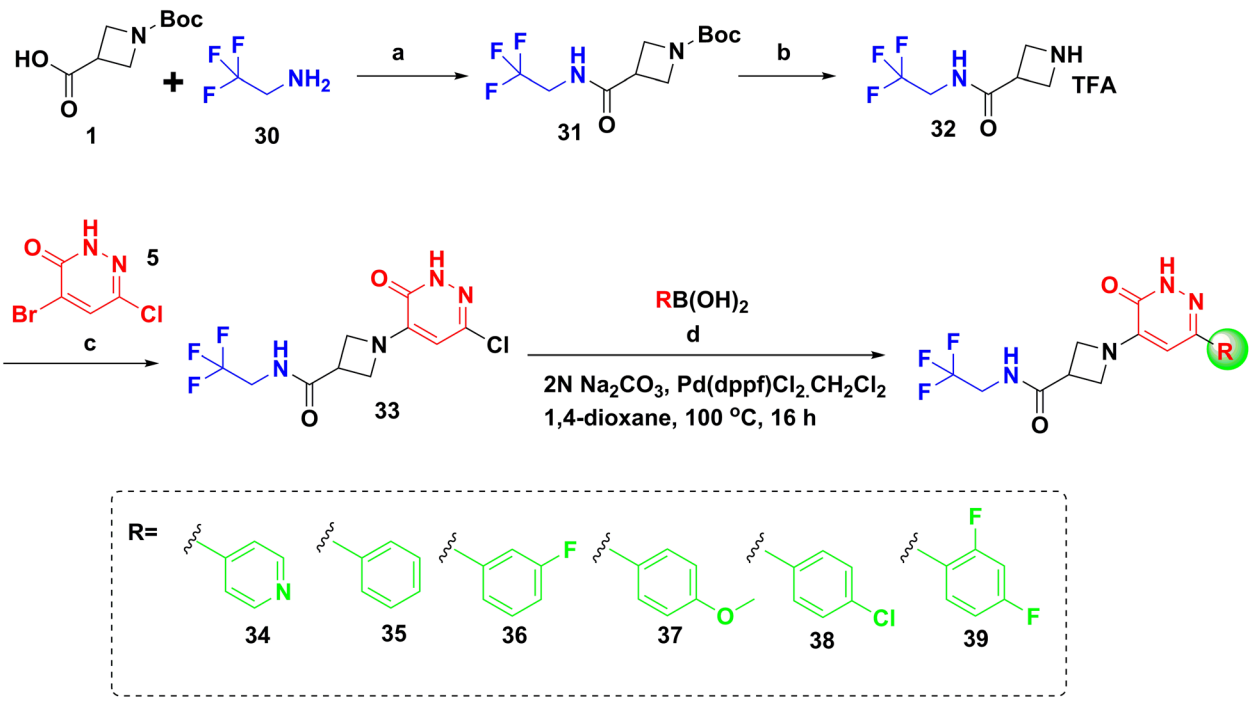

Scheme 4 Synthesis of compounds **34–39**. Reagents and conditions: (a) HATU, DIPEA, DMF, RT; (b) TFA, CH_2Cl_2, RT; (c) DIPEA, DMF, RT; (d) boronic acid, 2 N Na_2CO_3, $Pd(dppf)Cl_2 \cdot CH_2Cl_2$, 1,4-dioxane, 100 °C.

Table 4 Cytotoxicity of Scaffold 4 derivatives (compounds **34–39**) in cancer and non-cancer cell lines. IC_{50} values in μM (data are presented as the mean of ≥6 replicates). Therapeutic index (TI) was calculated using fibroblast cell lines: TI* = BJ/Jurkat; TI‡ = MRC-5/Jurkat

	ITK/BTK null				BTK positive		ITK positive		Non-cancer			
Cmpd	A549	HCT116	HCT116-p53	U2OS	RAMOS	K562	Jurkat	CCRF-CEM	BJ	MRC-5	TI*	TI‡
34	>50	>50	>50	>50	>50	>50	>50	>50	>50	>50	n. d.	n. d.
35	>50	>50	>50	>50	>50	>50	>50	>50	>50	>50	n. d.	n. d.
36	>50	>50	>50	>50	>50	>50	>50	>50	>50	>50	n. d.	n. d.
37	>50	>50	>50	>50	>50	>50	>50	>50	>50	>50	n. d.	n. d.
38	>50	>50	>50	>50	>50	>50	44.9	29.95	>50	>50	>1.11	>1.11
39	>50	>50	>50	>50	>50	>50	>50	26.75	>50	>50	n. d.	n. d.

43 furnished **44**, which underwent nucleophilic substitution with 4-bromo-6-chloropyridazin-3(2*H*)-one (**5**) to yield intermediate **45**. This was subjected to Suzuki coupling with pyridin-4-yl boronic acid to afford the final product, **46**.

2.6.2. Synthesis of scaffold 5b – compound 52. The synthesis of compound **52** is described in Scheme 6. *tert*-Butyl 3-(methoxy(methyl)carbamoyl)azetidine-1-carboxylate (**47**) was reacted with 1-bromo-4-fluorobenzene (**48**) to yield compound **49**, which was subsequently deprotected to obtain **50**. Nucleophilic substitution with 4-bromo-6-chloropyridazin-3(2*H*)-one (**5**) produced intermediate **51**, which underwent Suzuki coupling with pyridin-4-yl boronic acid to yield the final compound **52**.

Compound **46** exhibited moderate cytotoxic activity in ITK/BTK-expressing cells, with IC_{50} values of 35.9 μM in Jurkat and 29.03 μM in CCRF-CEM cells (Table 5). No cytotoxicity was

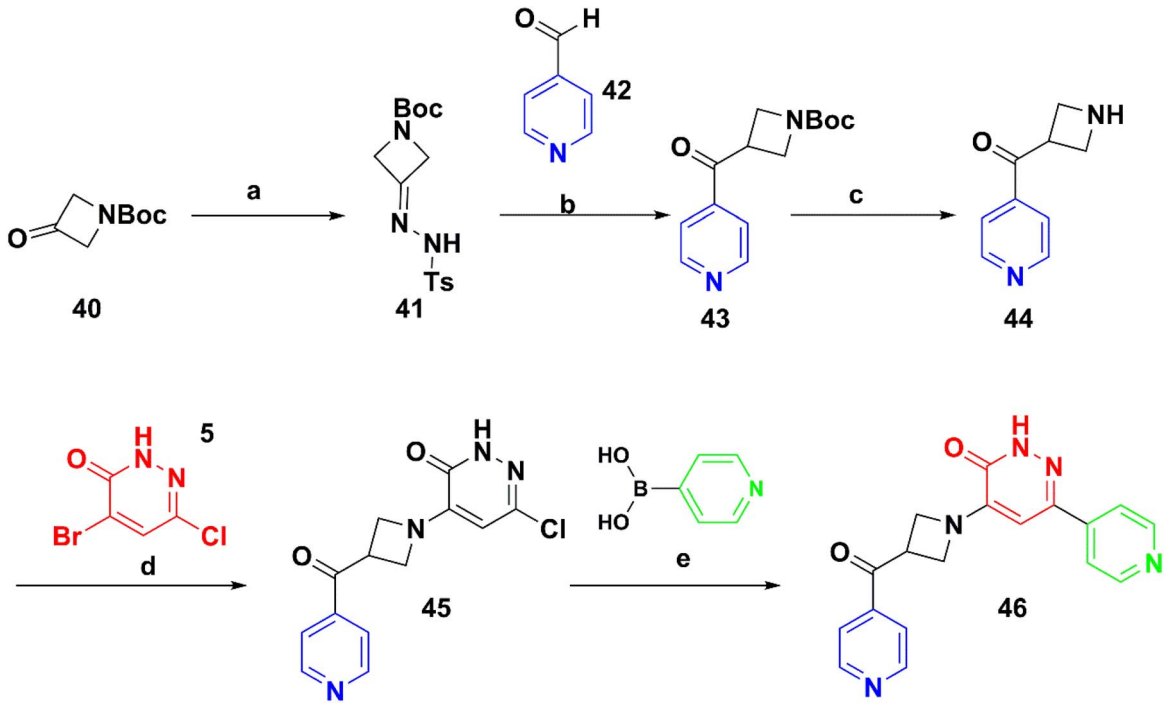

Scheme 5 Synthesis of compound **46**. Reagents and conditions: (a) $TsNHNH_2$, toluene, 110 °C; (b) **42**, Cs_2CO_3, 1,4-dioxane, 110 °C; (c) TFA, CH_2Cl_2, RT; (d) DIPEA, DMF, RT; (e) 2 N Na_2CO_3, $Pd(dppf)Cl_2 \cdot CH_2Cl_2$, 1,4-dioxane, 100 °C.

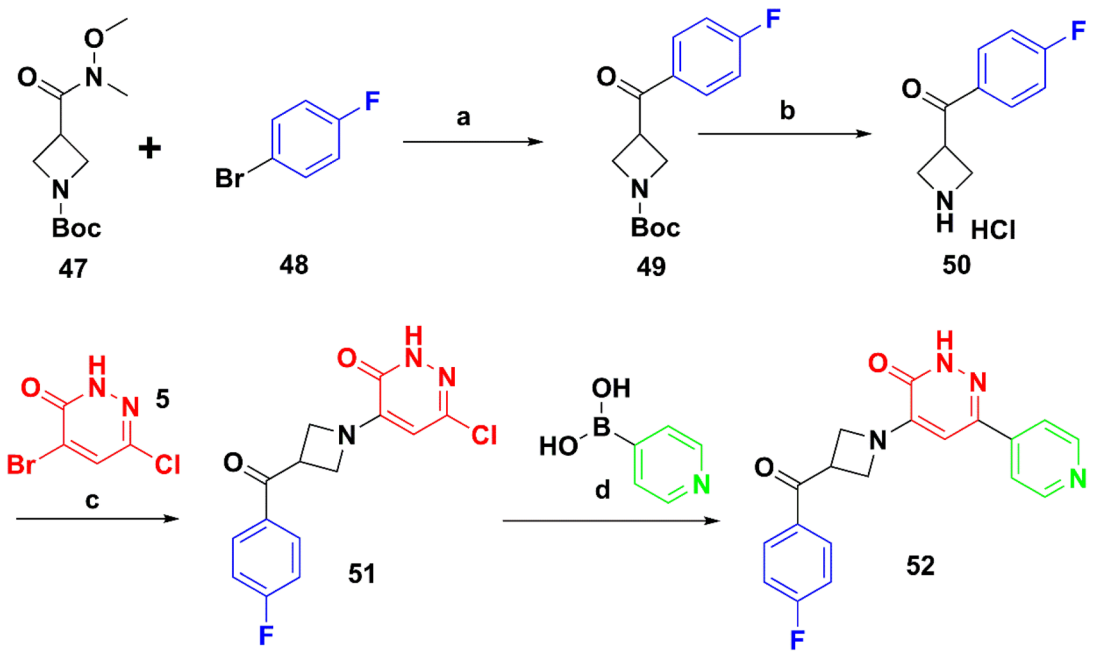

Scheme 6 Synthesis of compound **52**. Reagents and conditions: (a) *n*-BuLi, THF, −78 °C; (b) 4 M HCl in 1,4-dioxane, 0 °C; (c) DIPEA, DMF, RT; (d) 2 N Na_2CO_3, $Pd(dppf)Cl_2 \cdot CH_2Cl_2$, 1,4-dioxane, 100 °C.

observed in ITK-null (A549, HCT116, HCT116 p53, U2OS), BTK-positive (RAMOS, K562), or non-cancerous fibroblast cell lines (BJ, MRC-5), with IC_{50} values exceeding 50 μM across all tested lines. Compound **52** showed an IC_{50} of 20.7 μM in Jurkat cells and 13.24 μM in the BTK-positive RAMOS cell line. IC_{50} values in the remaining ITK-null, CCRF-CEM, and non-cancerous cell lines were >50 μM.

2.7 Docking analysis of selected compounds

Three representative compounds, **9**, **22**, and **23**, were selected for docking based on their observed cytotoxic activity in ITK/BTK-expressing cell lines. Molecular docking was performed *in silico* to evaluate the binding affinities and interaction profiles of these 3-oxo-2,3-dihydropyridazine derivatives against

Table 5 Different cell lines (compounds **46** and **52**) cytotoxicity of 3-oxo-2,3-dihydropyridazine derivatives (IC_{50} values in μM)

	ITK/BTK null				BTK positive		ITK positive		Non-cancer			
Cmpd	A549	HCT116	HCT116-p53	U2OS	RAMOS	K562	Jurkat	CCRF-CEM	BJ	MRC-5	TI*	TI‡
46	>50	>50	>50	>50	>50	>50	35.9	29.03	>50	>50	n. d.	n. d.
52	>50	>50	>50	>50	13.24	>50	20.7	—	>50	>50	n. d.	n. d.

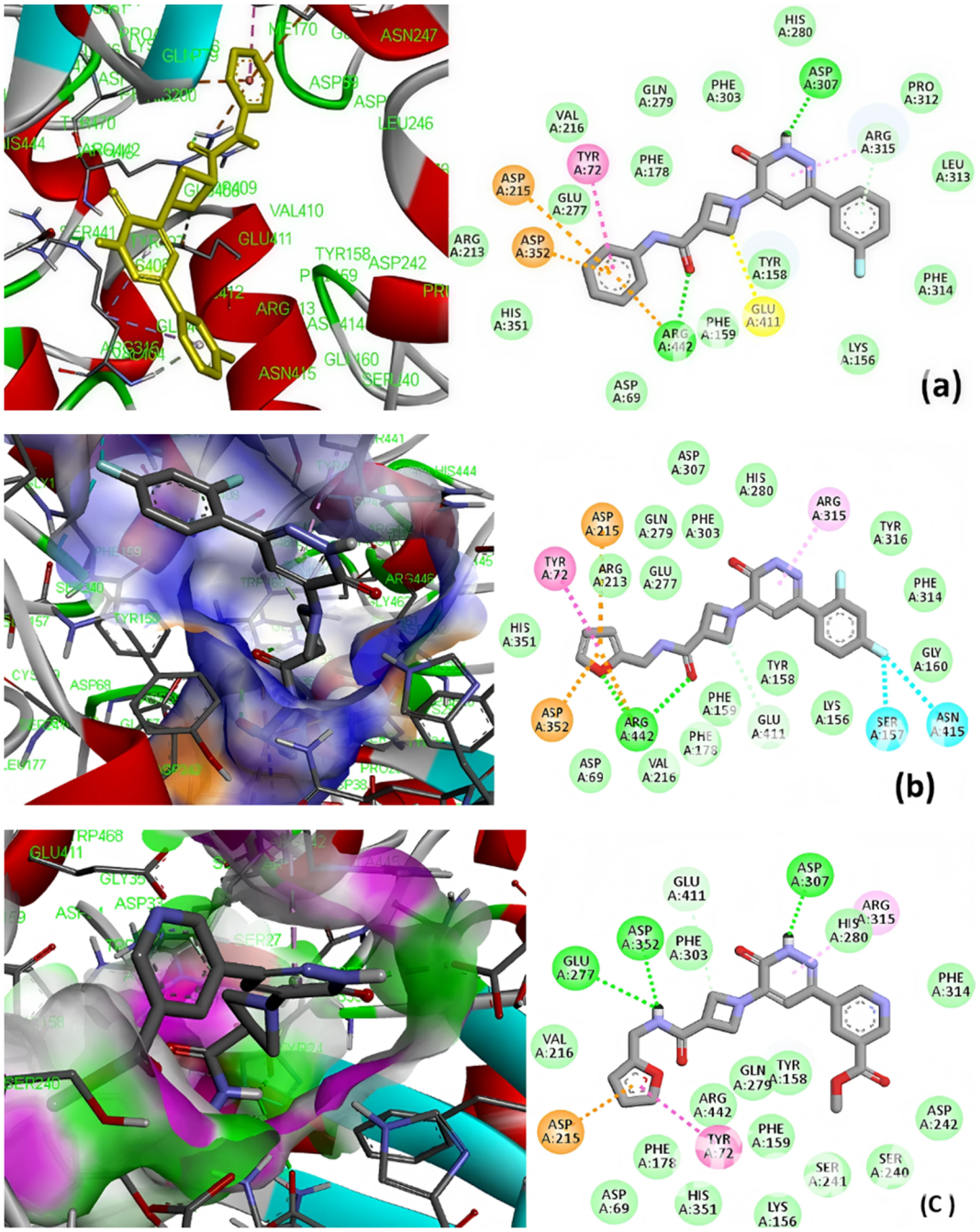

Fig. 2 Molecular docking interactions of (a) compound **9**, (b) compound **22**, (c) ompound **23** with ITK (PDB ID: 3QGW). 2D and 3D interaction diagrams are shown for compounds **9**, **22**, and **23** docked into the ITK active site. Hydrogen bonds are represented as green dashed lines, hydrophobic interactions in orange, and π-interactions in purple. Key interacting residues are labeled. Docking was performed using AutoDock Vina.

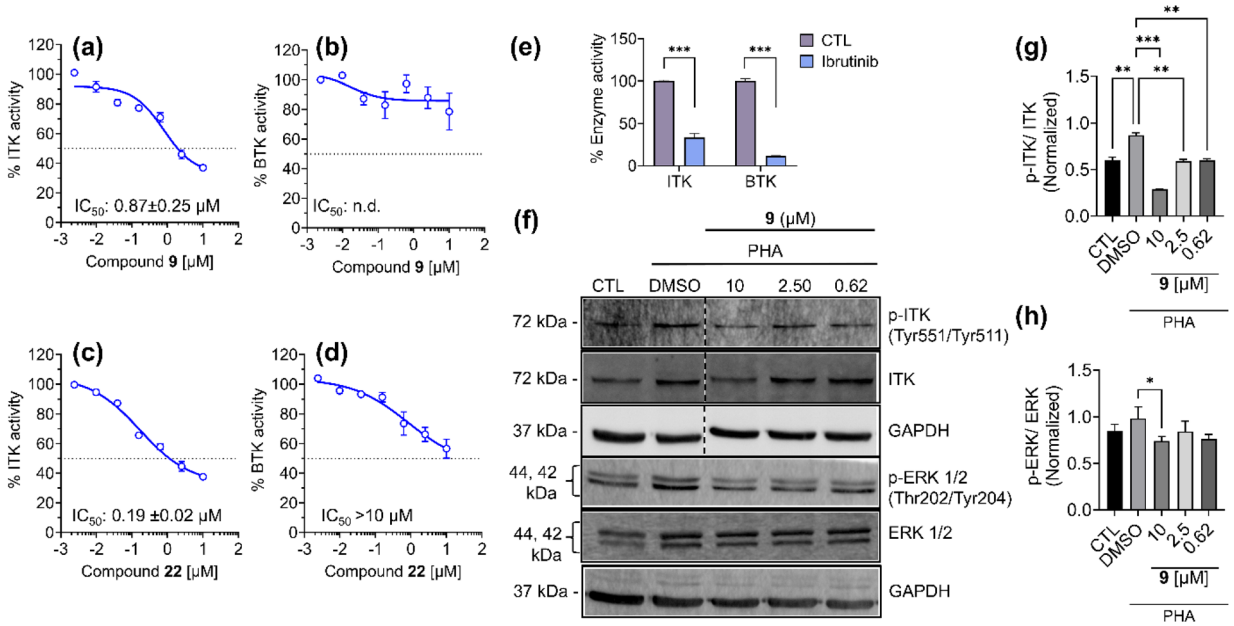

Fig. 3 Inhibition of ITK and BTK activity by compounds **9** and **22** (a–d) .

ITK using its crystal structure (PDB ID: 3QGW), co-crystallized with *N*-(6-oxo-1,6-dihydro-3,4-bipyridin-5-yl)benzamide (L7A), as the reference ligand. Among the tested compounds, **9** exhibited the highest binding affinity with a docking energy of −8.7 kcal mol^{-1}, followed by **22** (−8.6 kcal mol^{-1}) and **23** (−8.0 kcal mol^{-1}). All three compounds showed more favorable predicted binding energies than the reference ligands L7A and ibrutinib (Fig. 2).

Compound **9** was predicted to form conventional hydrogen bonds with Glu436, Met438, and Lys391 within the ITK active site. Compound **22** formed hydrogen bonds with Met438, Cys442, and Gly441, as well as a carbon–hydrogen bond with Lys391. It also engaged in van der waals interactions with Ser499, Val419, Phe435, Arg486, Gly370, Ile369, Phe437, and Glu436, and additional π–π-alkyl, π–π-sigma, and π–π-anion contacts with Ala389, Val377, Leu489, and Asp500. Compound **23**, although having slightly lower docking affinity, showed a strong binding profile, though the specific residues involved were not fully enumerated in the output. Detailed docking scores and protein–ligand interaction data for all compounds are summarized in the SI. These binding interactions highlight the complementarity between the 3-oxo-2,3-dihydropyridazine core and the ITK active site, consistent with the scaffold's design rationale.

The structural composition of these ligands included a 3-fluorophenyl group at the C-6 position and a phenyl substituent at the azetidine nitrogen in **9**; a 3,5-difluorophenyl ring at C-6 and a furan-2-ylmethyl substituent on the azetidine nitrogen in **22**; and a methyl nicotinate ester with a furan-2-ylmethyl group in **23**.

Overall, docking data corroborated the biological assays, supporting ITK as the primary molecular target of the most active compounds.

2.8 Biochemical kinase inhibition and western blot analysis

Next, compounds **9** and **22** were prioritized for kinase inhibition assays based on their overall performance in cytotoxicity screening, TI evaluation, and strong predicted ITK binding affinities from molecular docking studies. BTK was included as a closely related TEC-family off-target, given its high sequence homology with ITK within the TEC kinase family.[16]

Compound **9** inhibited ITK activity with an IC_{50} of 0.87 ± 0.25 μM (Fig. 3a), while showing no measurable inhibition of BTK (Fig. 3b). Compound **22** inhibited ITK with an IC_{50} of 0.19 ± 0.02 μM (Fig. 3c) and exhibited partial inhibition of BTK, with maximal inhibition not exceeding 50% at 10 μM (Fig. 3d). The effect of ibrutinib (100 μM) was used to validate assay performance, resulting in significant inhibition of both ITK and BTK activity (Fig. 3e).

To confirm protein-level effects, western blot analysis was performed in phytohemagglutinin (PHA)-stimulated Jurkat cells treated with **9**, which was selected for follow-up based on its selective ITK inhibition and absence of BTK inhibition in the kinase assay. A concentration-dependent decrease in p-ITK (Tyr551/Tyr511) was observed, with a modest reduction in total ITK at 10 μM (Fig. 3f and g). PHA-induced p-ERK1/2 (Thr202/Tyr204) levels were also reduced following treatment, with a significant decrease observed at the 10 μM concentration (Fig. 3f–h). Overall, densitometric analysis revealed a significant reduction in the p-ITK/ITK ratio at all concentrations tested and a significant decrease in the p-ERK/ERK ratio at the highest tested concentration. These biochemical and protein-level data together confirm that compound **9** directly inhibits ITK signaling rather than acting through nonspecific cytotoxic mechanisms.

Dose–response curves of compound **9** (a and b) and compound **22** (c and d) on ITK and BTK enzymatic activity,

respectively. Data represent mean ± standard error of the mean ($n = 3$), and IC_{50} values (μM) calculated from nonlinear regression are reported within each graph. For compound **22**, which showed a sigmoidal inhibition trend against BTK but without reaching >50% inhibition at 10 μM, the IC_{50} is reported as >10 μM. For **9**, no BTK inhibitory effect was observed, and the IC_{50} is indicated as n. d. (not determined). (e) Inhibition of ITK and BTK enzymatic activity by 100 μM ibrutinib. Mean ± standard error of the mean from 2–3 independent experiments; statistical significance *vs.* DMSO control was assessed by unpaired two-tailed t-test (**$p < 0.01$). (f) Western blot analysis of Jurkat cells stimulated with PHA (5 μg mL^{-1}) for 15 min, followed by treatment with **9** at the indicated concentrations for 24 h. CTL: untreated, unstimulated cells; DMSO: PHA-stimulated, DMSO-treated control. GAPDH was used as a loading control. Vertical dashed lines indicate non-contiguous lanes from the same blot. Uncropped images of blots are in the SI. (g and h) Quantification of p-ITK/ITK (g) and p-ERK/ERK (h) band intensities, calculated as the ratio of phosphorylated to total protein, and normalized to GAPDH. Mean ± standard error of the mean ($n = 2$), one-way ANOVA with Tukey's multiple comparisons test (***$p < 0.001$, **$p < 0.01$, *$p < 0.05$).

3. Discussion

This study identified a novel series of 3-oxo-2,3-dihydropyridazine derivatives with selective cytotoxicity toward ITK-expressing T-cell leukemia lines and promising ITK inhibitory profiles. To evaluate their therapeutic potential, we employed a combined approach that included scaffold-based synthesis, *in vitro* cytotoxicity profiling, kinase activity assays, molecular docking, and protein-level validation in relevant T-cell models.

Among the evaluated compounds, compound **9** demonstrated moderate cytotoxicity but showed high target selectivity in both kinase inhibition and cell-based assays. It showed no measurable BTK inhibition *in vitro* and was inactive in non-cancerous fibroblasts and ITK-null cancer lines, supporting a target-specific mechanism. These findings were corroborated by western blot analysis, which showed a concentration-dependent significant reduction in p-ITK levels and a significant decrease in p-ERK1/2 levels at the highest test concentration following treatment, confirming downstream pathway inhibition in Jurkat cells. The binding interactions of compound **9** in molecular docking further supported selective ITK engagement.

In contrast, compound **22** exhibited higher potency in both cytotoxicity and ITK kinase assays, as well as in docking interactions. However, its partial inhibition of BTK enzyme activity and cytotoxicity in BTK-expressing lines such as Ramos suggest potential off-target effects. While **22** maintained an acceptable TI, its reduced selectivity relative to **9** may limit its utility without further optimization.

Compound **23**, which showed appreciable cytotoxicity and high docking affinity, exhibited a broader activity profile, including cytotoxicity in non-cancerous and ITK-null cell lines, suggesting a lack of specificity. These observations underscore the crucial importance of integrating selectivity assessment with phenotypic screening when prioritizing kinase-directed agents.

It is also worth noting that several compounds with strong *in silico* docking scores, such as compound **29**, failed to exhibit corresponding biological activity. This underscores the limitations of docking as a predictive filter, particularly in the absence of supporting data on cell permeability, metabolic stability, or off-target effects.

While the present data demonstrates ITK-selective activity across cellular models with endogenous kinase expression, further studies using controlled ITK-knockdown or BTK-overexpression systems may refine mechanistic interpretation. Nonetheless, the activity pattern observed across ITK-positive, BTK-positive, and ITK/BTK-null cell lines provides strong evidence that the cytotoxic effects of the lead compounds reflect ITK-pathway engagement under physiologically relevant conditions.

Taken together, these results support the advancement of compound **9** as a selective ITK inhibitor with a favorable pharmacological profile. While our findings are promising, we acknowledge the need for additional studies to evaluate *in vivo* efficacy, metabolic stability, and broader kinase selectivity. Additional evaluation of apoptotic markers, mechanistic endpoints, and pathway effects will help strengthen the therapeutic rationale and translational relevance of this compound series.

4. Conclusion

This study led to the identification of selective ITK inhibitors from a newly synthesized library of 3-oxo-2,3-dihydropyridazine derivatives. Compound **9** was prioritized based on its selective inhibition of ITK, absence of BTK activity, low off-target cytotoxicity, and favorable TI. Compound **22** also showed potent ITK inhibition but exhibited partial activity against BTK, and demonstrated a selective reduction in relevant cell lines. While both compounds represent valuable leads, further optimization of **22** may be necessary to improve its kinase selectivity. Overall, these findings lay the groundwork for advancing compound **9** into additional pharmacological studies and support its potential as a selective ITK inhibitor for further preclinical development.

5. Experimental procedure

5.1 Materials and physical measurements

All chemical reagents were obtained from Lancaster (Alfa Aesar, Johnson Matthey Co., Ward Hill, MA, USA), Sigma-Aldrich (St. Louis, MO, USA), and Spectrochem Pvt. Ltd. (Mumbai, India). The aryl boronic acids were obtained from Combi-Blocks, Inc., San Diego, CA, USA. Reaction progress was monitored using thin-layer chromatography (TLC) on silica gel-coated aluminum plates with a fluorescent indicator (F254S). Spots were visualized under UV light and by applying potassium permanganate or iodine staining.

Proton (^{1}H) and carbon (^{13}C) nuclear magnetic resonance (NMR) spectra were recorded on a Bruker ascend 400 MHz NMR spectrometer (Billerica, MA, USA), with chemical shifts reported

in parts per million (ppm) relative to an internal tetramethylsilane (TMS) reference. Signal multiplicities are described using the following abbreviations: s (singlet), d (doublet), dd (doublet of doublets), t (triplet), td (triplet of doublets), bs (broad singlet), and m (multiplet). Electrospray ionization (ESI) mass spectra were recorded on a MicroMass Quattro LC system (Waters, Milford, MA, USA) operating in positive ion mode, with a capillary voltage of 3.98 kV and processed using ESI+ software. Infrared (IR) spectra were acquired using an IR Affinity-1S FT-IR spectrometer (Shimadzu, Japan), with only the principal absorption bands (in cm^{-1}) reported. All sample solutions were prepared using deionized distilled water, and other reagents used were commercially available and of analytical grade. The melting point was determined using a BUCHI M-565 (Flawil, Switzerland) melting point apparatus.

5.2 Chemistry

The synthesis of target compounds **7–12** were outlined in Scheme 1. For these compounds ^{1}H NMR chemical shift value of the pyridazine –NH proton was appeared as a singlet between δ 12.6–12.7 ppm, phenyl amide –NH was observed as a singlet at δ 10.1 ppm, azetidine –CH_2 protons were appeared as a multiplet at δ 4.45–4.35 ppm, aromatic protons were appeared at ranging from δ 8.65–6.55 ppm. Azetidine –CH proton was appeared at δ 3.7–3.65 ppm. The synthesis of target compounds **17–23** were outlined in Scheme 2. For these compounds ^{1}H NMR chemical shift value of the pyridazine –NH proton was observed as a singlet between δ 12.7–12.4 ppm, Phenyl amide –NH was observed at δ 8.5 ppm, azetidine –CH_2 protons were between at δ 4.35–4.25 ppm, aromatic protons were appeared at ranging from δ 8.65–6.55 ppm. Azitidine –CH protons were appeared as a multiplet at δ 3.55–3.65 ppm. Furan attached –CH_2 proton was appeared at δ 4.30 ppm. The synthesis of target compounds **28** and **29** are outlined in Scheme 3. For these compounds ^{1}H NMR chemical shift value of the phenylpiperazine protons were observed between δ 3.64–3.13 ppm. The synthesis of target compounds 34–39 were outlined in Scheme 4. For these compounds trifluoro attached CH_2 proton was appeared at δ 3.9 ppm. For compound **46** (Scheme 5), ^{1}H NMR chemical shift value of the both pyridine aromatic protons were appeared as doublets between δ 8.86–8.62 ppm. Pyridazine ring –CH proton was observed as a singlet at δ 6.60 ppm. For compound **52** (Scheme 6), ^{1}H NMR chemical shift value of the pyridine aromatic protons were appeared as doublets between δ 8.63–7.99 ppm. Fluorine substituted aromatic protons were appeared between δ 7.82–7.38 ppm.

5.2.1. General procedure for amide coupling. To a stirred solution of 1-(*tert*-butoxycarbonyl)azetidine-3-carboxylic acid (1.0 equiv.) in DMF (5–10 v) at 0 °C under nitrogen atmosphere were added DIPEA (3.0 equiv.), HATU (1.3 equiv.) and amine (1.1 equiv.). The resulting reaction mixture was stirred at RT for 16 h. The progress of the reaction was monitored by TLC. The reaction mixture was diluted with water (50 mL) and extracted with EtOAc (2 × 100 mL). The combined organic layer was washed with brine (2 × 30 mL), dried over anhydrous sodium sulphate, filtered and concentrated under reduced pressure to get the crude product, which upon purification by flash chromatography (using Biotage, Claricep, silica cartridge, eluted with 35–40% of EtOAc in petether). The pure fractions were concentrated under reduced pressure.

5.2.2. General procedure for Boc deprotection. To a stirred solution of *tert*-butyl azetidine-1-carboxylate (1.0 equiv.) in CH_2Cl_2 (10 v) was added TFA (5.0 equiv.) at 0 °C. The resulting reaction mixture was stirred at RT for 2 h. The progress of the reaction was monitored by TLC and LC-MS. After completion of the reaction, the reaction mixture was concentrated under reduced pressure, and the residue was triturated with diethyl ether and dried under vacuum to get the product as a TFA salt.

5.2.3. General procedure for substitution reaction. To a stirred solution of TFA salt (1.0 equiv.) in DMF (10 mL) was added 4-bromo-6-chloropyridazin-3(2*H*)-one (1.0 equiv.) and DIPEA (3 equiv.) at 0 °C under a nitrogen atmosphere, and the reaction mixture was allowed to stir at RT for 16 h. The progress of the reaction was monitored by TLC. The reaction mixture was diluted with ice-cold water and filtered. The resulting solid was washed with water and dried under vacuum to afford the 6-chloro-3-oxo-2,3-dihydropyridazin derivative.

5.2.4. General procedure for Suzuki coupling reaction. To a stirred solution of 6-chloro-3-oxo-2,3-dihydropyridazin derivative (1.0 equiv.) in 1,4-dioxane (10 mL) were added 2 N Na_2CO_3 (3.0 equiv.), pyridin-4-yl boronic acid (1.3 equiv.) and degassed with argon for 5 minutes before the addition of Pd(dppf)Cl_2-·CH_2Cl_2 (0.1 equiv.) was stirred at 100 °C for 16 h. The reaction mixture was diluted with ice-cold water (30 mL) and extracted with EtOAc (2 × 50 mL). The combined organic layer was washed with brine (20 mL), dried over anhydrous Na_2SO_4, filtered and concentrated under reduced pressure to afford crude compound, which upon purification by flash chromatography (using Biotage, Claricep, 12 g silica cartridge, eluted with 5–10% of MeOH in CH_2Cl_2) to afford the final product.

*5.2.4.1. Preparation of tert-butyl 3-(phenylcarbamoyl) azetidine-1-carboxylate (**3**).*[17] To a stirred solution of 1-(*tert*-butoxycarbonyl)azetidine-3-carboxylic acid **1** (3 g, 14.909 mmol, 1 equiv.) in DMF (20 mL) at 0 °C under a nitrogen atmosphere, were added DIPEA (7.69 mL, 44.727 mmol, 3 equiv.), HATU (7.6 g, 19.38 mmol, 1.3 equiv.) and aniline **2** (1.52 g, 16.399 mmol, 1.1 equiv.). The resulting reaction mixture was stirred at RT for 16 h. The progress of the reaction was monitored by TLC. The reaction mixture was diluted with water (50 mL) and then extracted with ethyl acetate (EtOAc) (2 × 100 mL). The combined organic layer was washed with brine (2 × 30 mL), dried over anhydrous sodium sulphate, filtered, and concentrated under reduced pressure to get the crude product, which upon purification by flash chromatography (using Biotage, Claricep, 80 g silica cartridge, eluted with 35–40% of EtOAc in petether) to afford (3.6 g, 13.13 mmol, 87%) *tert*-butyl 3-(phenylcarbamoyl)azetidine-1-carboxylate **3** as a pale-yellow solid. ^{1}H-NMR (400 MHz, $CDCl_3$): δ 7.52 (d, J = 8.0 Hz, 2H), 7.33 (t, J = 7.6 Hz, 3H), 7.13 (t, J = 7.2 Hz, 1H), 4.23–4.19 (m, 2H), 4.11 (t, J = 8.4 Hz, 2H), 3.36–3.31 (m, 1H); 1.45 (s, 9H); LC-MS (ES-API): m/z = 275.08 $(M-H)^+$, 95.1% purity by LC-MS.

*5.2.4.2. Preparation of N-phenylazetidine-3-carboxamide (**4**).* To a stirred solution of *tert*-butyl 3-(phenylcarbamoyl)azetidine-

1-carboxylate **3** (3.6 g, 13.02 mmol) in CH_2Cl_2 (36 mL) was added TFA (4.95 mL, 65.13 mmol, 5.0 equiv.) at 0 °C. The resulting reaction mixture was stirred at RT for 2 h. The progress of the reaction was monitored by TLC and LC-MS. After completion of the reaction, the reaction mixture was concentrated under reduced pressure, and the residue was triturated with diethyl ether (30 mL). The resulting solid was then dried under vacuum to yield 3.4 g (19.3 mmol, 95%) of *N*-phenylazetidine-3-carboxamide **4** (TFA salt) as a pale yellow solid. LC-MS (ES-API): $m/z = 177.46$ $(M + H)^+$, 87% purity by LC-MS.

*5.2.4.3. Preparation of 1-(6-chloro-3-oxo-2,3-dihydropyridazin-4-yl)-N-phenylazetidine-3-carboxamide (**6**).* To a stirred solution of *N*-phenylazetidine-3-carboxamide **4** (TFA salt) (3.4 g, 12.39 mmol, 1.0 equiv.) in DMF (34 mL) were added 4-bromo-6-chloropyridazin-3(2*H*)-one **5** (2.59 g, 12.39 mmol, 1.0 equiv.) and DIPEA (6.39 mL, 37.17 mmol, 3 equiv.) at 0 °C under nitrogen atmosphere and allowed the reaction mixture to stir at RT for 16 h. The progress of the reaction was monitored by TLC. The reaction mixture was diluted with ice-cold water (50 mL) and filtered. The resulting solid was washed with water (20 mL) and dried under vacuum to afford (3.1 g, 10.19 mmol, 82%) 1-(6-chloro-3-oxo-2,3-dihydropyridazin-4-yl)-*N*-phenylazetidine-3-carboxamide **6** as a pale-yellow solid. LC-MS (ES-API): $m/z = 305.0$ $(M + H)^+$, 75.9% purity by LC-MS.

5.2.4.4. Preparation of 1-(3-oxo-6-(pyridin-4-yl)-2,3-dihydropyridazin-4-yl)-N-phenylazetidine-3-carboxamide (7).[18] To a stirred solution of 1-(6-chloro-3-oxo-2,3-dihydropyridazin-4-yl)-*N*-phenylazetidine-3-carboxamide **6** (200 mg, 0.656 mmol, 1.0 equiv.) in 1,4-dioxane (10 mL) were added 2 N Na_2CO_3 (208 mg, 1.968 mmol, 3.0 equiv.), pyridin-4-yl boronic acid (104.8 mg, 0.853 mmol, 1.3 equiv.) and degassed with argon for 5 minutes before the addition of $Pd(dppf)Cl_2 \cdot CH_2Cl_2$ (54 mg, 0.065 mmol, 0.1 equiv.) was stirred at 100 °C for 16 h. The reaction mixture was diluted with ice-cold water (30 mL) and extracted with EtOAc (2 × 50 mL). The combined organic layer was washed with brine (20 mL), dried over anhydrous Na_2SO_4, filtered and concentrated under reduced pressure to afford crude compound, which upon purification by flash chromatography (using Biotage, Claricep, 12 g silica cartridge, eluted with 5–10% of MeOH in CH_2Cl_2) to afford (18 mg, 0.052 mmol, 8%) 1-(3-oxo-6-(pyridin-4-yl)-2,3-dihydropyridazin-4-yl)-*N*-phenylazetidine-3-carboxamide 7 as an off-white solid. ^{1}H NMR (400 MHz, DMSO-d_6): δ 12.77 (s, 1H), 10.11 (s, 1H), 8.63 (d, $J =$ 6.0 Hz, 2H), 7.82 (d, $J = 6.0$ Hz, 2H), 7.62 (d, $J = 7.6$ Hz, 2H), 7.31 (t, $J = 7.6$ Hz, 2H), 7.05 (t, $J = 7.6$ Hz, 1H), 6.55 (s, 1H), 4.36–4.34 (m, 4H), 3.62–3.72 (m, 1H); ^{13}C-NMR (400 MHz, DMSO-d_6): 196.9, 170.2, 156.6, 150.0, 145.1, 143.1, 138.9, 128.7, 123.3, 119.9, 119.2, 98.2, 35.1. IR: 1639.4 cm^{-1} (C═O stretching); LC-MS (ES-API): $m/z = 348.1$ $(M + H)^+$; purity by HPLC: 96.8%; MR: 243–246 °C.

*5.2.4.5. Preparation of 1-(3-oxo-6-phenyl-2,3-dihydropyridazin-4-yl)-N-phenylazetidine-3-carboxamide (**8**).* To a stirred solution of 1-(6-chloro-3-oxo-2,3-dihydropyridazin-4-yl)-*N*-phenylazetidine-3-carboxamide **6** (200 mg, 0.656 mmol, 1.0 equiv.) in 1,4-dioxane (10 mL) were added 2 N Na_2CO_3 (208 mg, 1.968 mmol, 3.0 equiv.), phenylboronic acid (104.8 mg, 0.853 mmol, 1.3 equiv.) and degassed with argon for 5 minutes before the addition of $Pd(dppf)Cl_2 \cdot CH_2Cl_2$ (54 mg, 0.065 mmol, 0.1 equiv.) was stirred at 100 °C for 16 h. The reaction mixture was diluted with ice-cold water (30 mL) and then extracted with ethyl acetate (EtOAc) (2 × 50 mL). The combined organic layer was washed with brine (20 mL), dried over anhydrous Na_2SO_4, filtered and concentrated under reduced pressure to afford crude compound, which upon purification by flash chromatography (using Biotage, Claricep, 12 g silica cartridge, eluted with 5–10% of MeOH in CH_2Cl_2) to afford (22 mg, 0.063 mmol, 10%) 1-(3-oxo-6-phenyl-2,3-dihydropyridazin-4-yl)-*N*-phenylazetidine-3-carboxamide **8** as a light brown solid. ^{1}H-NMR (400 MHz, DMSO-d_6): δ 12.56 (s, 1H), 10.09 (s, 1H), 7.83 (d, $J = 7.6$ Hz, 2H), 7.62 (d, $J = 7.6$ Hz, 2H), 7.45–7.37 (m, 3H), 7.31 (t, $J = 7.6$ Hz, 2H), 7.05 (t, $J = 7.2$ Hz, 1H), 6.44 (s, 1H), 4.41–4.33 (m, 4H), 3.70–3.66 (m, 1H); ^{13}C-NMR (400 MHz, DMSO-d_6): 170.3, 156.5, 145.4, 145.1, 139.0, 136.1, 128.7, 128.6, 128.5, 125.7, 123.3, 119.2, 99.0, 35.1; IR: 1654.9 cm^{-1} (C═O stretching), LC-MS (ES-API): $m/z = 347.13$ $(M + H)^+$; purity by HPLC: 91.7%; MR: 270–273 °C.

*5.2.4.6. Preparation of 1-(6-(3-fluorophenyl)-3-oxo-2,3-dihydropyridazin-4-yl)-N-phenylazetidine-3-carboxamide (**9**).* To a stirred solution of 1-(6-chloro-3-oxo-2,3-dihydropyridazin-4-yl)-*N*-phenylazetidine-3-carboxamide **6** (200 mg, 0.656 mmol, 1.0 equiv.) in 1,4-dioxane (10 mL) were added 2 N Na_2CO_3 (208 mg, 1.968 mmol, 3.0 equiv.), (3-fluorophenyl)boronic acid (119.4 mg, 0.853 mmol, 1.3 equiv.) and degassed with argon for 5 minutes prior to the addition of $Pd(dppf)Cl_2 \cdot CH_2Cl_2$ (54 mg, 0.065 mmol, 0.1 equiv.) was stirred at 100 °C for 16 h. The reaction mixture was diluted with ice-cold water (30 mL) and then extracted with ethyl acetate (EtOAc) (2 × 50 mL). The combined organic layer was washed with brine (20 mL), dried over anhydrous Na_2SO_4, filtered, and concentrated under reduced pressure to afford crude compound, which, upon purification by flash chromatography (using Biotage, Claricep, 12 g silica cartridge, eluted with 5–10% of MeOH in CH_2Cl_2) to afford (35 mg, 0.096 mmol, 15%) 1-(6-(3-fluorophenyl)-3-oxo-2,3-dihydropyridazin-4-yl)-*N*-phenylazetidine-3-carboxamide **9** as a light brown solid. ^{1}H-NMR (500 MHz, DMSO-d_6): δ 12.65 (s, 1H), 10.06 (s, 1H), 7.70–7.59 (m, 4H), 7.52–7.45 (m, 1H), 7.31 (t, $J =$ 7.5 Hz, 2H), 7.23 (t, $J = 8.0$ Hz, 1H), 7.05 (t, $J = 7.0$ Hz, 1H), 6.49 (s, 1H), 4.62–4.21 (m, 4H), 3.69–3.66 (m, 1H); ^{13}C-NMR (400 MHz, DMSO-d_6): 170.7, 164.1, 161.7, 157.0, 145.5, 144.7, 139.4, 139.1, 139.0, 131.0, 130.9, 129.9, 129.2, 123.8, 122.2, 120.4, 120.3, 119.7, 117.3, 117.1, 115.9, 115.7, 113.0, 112.8, 99.3; IR: 1656.8 cm^{-1} (C═O stretching), LC-MS (ES-API): $m/z = 365.13$ $(M + H)^+$; purity by HPLC: 93.2%; MR: 255–258 °C.

*5.2.4.7. Preparation of 1-(6-(4-methoxyphenyl)-3-oxo-2,3-dihydropyridazin-4-yl)-N-phenylazetidine-3-carboxamide (**10**).* To a stirred solution of 1-(6-chloro-3-oxo-2,3-dihydropyridazin-4-yl)-*N*-phenylazetidine-3-carboxamide **6** (200 mg, 0.656 mmol, 1.0 equiv.) in 1,4-dioxane (10 mL) were added 2 N Na_2CO_3 (208 mg, 1.968 mmol, 3.0 equiv.), (4-methoxyphenyl)boronic acid (129.5 mg, 0.853 mmol, 1.3 equiv.) and degassed with argon for 5 minutes before the addition of $Pd(dppf)Cl_2 \cdot CH_2Cl_2$ (54 mg, 0.065 mmol, 0.1 equiv.), and stirred 100 °C for 16 h. The reaction mixture was diluted with ice-cold water (30 mL) and then extracted with ethyl acetate (EtOAc) (2 × 50 mL). The

combined organic layer was washed with brine (20 mL), dried over anhydrous Na_2SO_4, filtered, and concentrated under reduced pressure to afford crude compound, which, upon purification by flash chromatography (using Biotage, Claricep, 12 g silica cartridge, eluted with 5–10% of MeOH in CH_2Cl_2) to afford (36 mg, 0.095 mmol, 15%) 1-(6-(4-methoxyphenyl)-3-oxo-2,3-dihydropyridazin-4-yl)-*N*-phenylazetidine-3-carboxamide **10** as an off-white solid. ^{1}H-NMR (400 MHz, DMSO-d_6): δ 12.46 (s, 1H), 10.06 (s, 1H), 7.76 (d, J = 8.8 Hz, 2H), 7.62 (d, J = 7.6 Hz, 2H), 7.31 (t, J = 7.6 Hz, 2H), 7.05 (t, J = 7.2 Hz, 1H), 6.98 (d, J = 8.8 Hz, 2H), 6.40 (s, 1H), 4.40–4.31 (m, 4H), 3.79 (s, 3H), 3.69–3.64 (m, 1H); ^{13}C-NMR (400 MHz, DMSO-d_6): 170.3, 159.7, 156.4, 145.2, 145.0, 138.9, 128.7, 128.6, 127.1, 123.3, 119.2, 113.9, 98.9, 55.1, 35.1; IR: 1653.0 cm^{-1} (C=O stretching); LC-MS (ES-API): m/z = 377.15 (M + H)$^+$; purity by HPLC: 98.04%; MR: 256–258 °C.

*5.2.4.8. Preparation of 1-(6-(4-chlorophenyl)-3-oxo-2,3-dihydropyridazin-4-yl)-N-phenylazetidine-3-carboxamide (**11**).* To a stirred solution of 1-(6-chloro-3-oxo-2,3-dihydropyridazin-4-yl)-*N*-phenylazetidine-3-carboxamide **6** (200 mg, 0.656 mmol, 1.0 equiv.) in 1,4-dioxane (10 mL) were added 2 N Na_2CO_3 (208 mg, 1.968 mmol, 3.0 equiv.), (4-chlorophenyl)boronic acid (133.8 mg, 0.853 mmol, 1.3 equiv.) and degassed with argon for 5 minutes before the addition of Pd(dppf)$Cl_2\cdot CH_2Cl_2$ (54 mg, 0.065 mmol, 0.1 equiv.) was stirred at 100 °C for 16 h. The reaction mixture was diluted with ice-cold water (30 mL) and then extracted with ethyl acetate (EtOAc) (2 × 50 mL). The combined organic layer was washed with brine (20 mL), dried over anhydrous Na_2SO_4, filtered and concentrated under reduced pressure to afford crude compound, which upon purification by flash chromatography (using Biotage, Claricep, 12 g silica cartridge, eluted with 5–10% of MeOH in CH_2Cl_2) to afford (45 mg, 0.118 mmol, 18%) 1-(6-(4-chlorophenyl)-3-oxo-2,3-dihydropyridazin-4-yl)-*N*-phenylazetidine-3-carboxamide **11** as an off-white solid. ^{1}H-NMR (500 MHz, DMSO-d_6): δ 12.60 (s, 1H), 10.06 (s, 1H), 7.86 (d, J = 8.5 Hz, 2H), 7.62 (d, J = 7.5 Hz, 2H), 7.49 (t, J = 9.0 Hz, 2H), 7.31 (t, J = 9.5 Hz, 2H), 7.05 (t, J = 7.0 Hz, 1H), 6.45 (s, 1H), 4.49–4.21 (m, 4H), 3.70–3.64 (m, 1H); ^{13}C-NMR (400 MHz, DMSO-d_6): 170.2, 156.5, 145.0, 144.3, 138.9, 134.9, 133.3, 130.7, 130.2, 128.7, 127.5, 123.3, 119.2, 98.6, 55.3, 35.1; IR: 1660.7 cm^{-1} (C=O stretching); LC-MS (ES-API): m/z = 381.08 (M + H)$^+$; purity by HPLC: 94.6%; MR: 258–261 °C.

*5.2.4.9. Preparation of 1-(6-(2,4-difluorophenyl)-3-oxo-2,3-dihydropyridazin-4-yl)-N-phenylazetidine-3-carboxamide (**12**).* To a stirred solution of 1-(6-chloro-3-oxo-2,3-dihydropyridazin-4-yl)-*N*-phenylazetidine-3-carboxamide **6** (200 mg, 0.656 mmol, 1.0 equiv.) in 1,4-dioxane (10 mL) were added 2 N Na_2CO_3 (208 mg, 1.968 mmol, 3.0 equiv.), (2,4-difluorophenyl)boronic acid (134.7 mg, 0.853 mmol, 1.3 equiv.) and degassed with argon for 5 minutes before the addition of Pd(dppf)$Cl_2\cdot CH_2Cl_2$ (54 mg, 0.065 mmol, 0.1 equiv.) was stirred at 100 °C for 16 h. The reaction mixture was diluted with ice-cold water (30 mL) and extracted with EtOAc (2 × 50 mL). The combined organic layer was washed with brine (20 mL), dried over anhydrous Na_2SO_4, filtered and concentrated under reduced pressure to afford crude compound, which upon purification by flash chromatography (using Biotage, Claricep, 12 g silica cartridge, eluted with 5–10% of MeOH in CH_2Cl_2) to afford (41 mg, 0.107 mmol, 16%) 1-(6-(2,4-difluorophenyl)-3-oxo-2,3-dihydropyridazin-4-yl)-*N*-phenylazetidine-3-carboxamide **12** as an off-white solid. ^{1}H-NMR (400 MHz, DMSO-d_6): δ 12.68 (s, 1H), 10.06 (s, 1H), 7.70–7.60 (m, 3H), 7.38–7.29 (m, 3H), 7.18 (d, J = 8.0 Hz, 1H), 7.05 (t, J = 7.6 Hz, 1H), 6.17 (d, J = 1.6 Hz, 1H), 4.37–4.30 (m, 4H), 3.73–3.62 (m, 1H); ^{13}C-NMR (400 MHz, DMSO-d_6): 170.2, 163.6, 163.5, 161.1, 161.0, 160.8, 160.7, 158.3, 158.2, 156.3, 144.6, 142.0, 138.9, 131.4, 131.3, 128.7, 128.5, 128.5, 128.4, 123.3, 121.5, 121.4, 119.2, 111.9, 111.7, 104.8, 104.5, 104.3, 101.5, 101,4, 54.8, 35.1; IR: 1654.97 cm^{-1} (C=O stretching); LC-MS (ES-API): m/z = 383.11 (M + H)$^+$; purity by HPLC: 96%; MR: 260–263 °C.

*5.2.4.10. Preparation of tert-butyl 3-((furan-2-ylmethyl) carbamoyl)azetidine-1-carboxylate (**14**).* To a stirred solution of 1-(*tert*-butoxycarbonyl)azetidine-3-carboxylic acid **1** (3 g, 14.909 mmol, 1 equiv.) in DMF (20 mL) at 0 °C under nitrogen atmosphere were added DIPEA (7.69 mL, 44.727 mmol, 3 equiv.), HATU (7.6 g, 19.38 mmol, 1.3 equiv.) and furan-2-ylmethanamine **13** (1.59 g, 16.399 mmol, 1.1 equiv.). The resulting reaction mixture was stirred at RT for 16 h. The progress of the reaction was monitored by TLC. The reaction mixture was diluted with water (50 mL) and then extracted with ethyl acetate (EtOAc) (2 × 100 mL). The combined organic layer was washed with brine (2 × 30 mL), dried over anhydrous sodium sulphate, filtered and concentrated under reduced pressure to get the crude product, which upon purification by flash chromatography (using Biotage, Claricep, 80 g silica cartridge, eluted with 35–40% of EtOAc in petether) to afford (3.5 g, 12.5 mmol, 84%) *tert*-butyl 3-((furan-2-ylmethyl) carbamoyl)azetidine-1-carboxylate **14** as a pale-yellow solid. ^{1}H-NMR (400 MHz, $CDCl_3$): δ 7.35 (dd, J = 1.6 Hz, J = 0.8 Hz, 1H), 6.32 (dd, J = 3.2 Hz, J = 2.0 Hz, 1H), 6.23 (dd, J = 3.2 Hz, J = 0.8 Hz, 1H), 6.05 (br s, 1H), 4.45 (d, J = 5.6 Hz, 2H), 4.10 (t, J = 7.2 Hz, 2H), 4.02 (t, J = 8.8 Hz, 2H), 3.23–3.15 (m, 1H), 2.79 (s, 4H); 1.43 (s, 9H); LC-MS: (ES-API): m/z = 281.14 (M + H)$^+$, 99% purity by LC-MS.

*5.2.4.11. Preparation of N-(furan-2-ylmethyl)azetidine-3-carboxamide (**15**).* To a stirred solution of *tert*-butyl 3-((furan-2-ylmethyl)carbamoyl)azetidine-1-carboxylate **14** (3.5 g, 12.48 mmol, 1 equiv.) in CH_2Cl_2 (35 mL) was added TFA (4.8 mL, 62.42 mmol, 5.0 equiv.) at 0 °C. The resulting reaction mixture was stirred at RT for 2 h. The progress of the reaction was monitored by TLC and LC-MS. After completion of the reaction, the reaction mixture was concentrated under reduced pressure, and the residue was triturated with diethyl ether (30 mL). The resulting solid was dried under vacuum to yield 3.2 g (93%) of *N*-(furan-2-ylmethyl)azetidine-3-carboxamide 15 (as the TFA salt) as a pale-yellow solid. LC-MS (ES-API): m/z = 181.11 (M + H)$^+$, purity by LC-MS: 75.5%.

*5.2.4.12. Preparation of 1-(6-chloro-3-oxo-2,3-dihydropyridazin-4-yl)-N-(furan-2-ylmethyl)azetidine-3-carboxamide (**16**).* To a stirred solution of *N*-(furan-2-ylmethyl) azetidine-3-carboxamide **15** (3.2 g, 11.5 mmol, 1.0 equiv.) in DMF (34 mL) were added 4-bromo-6-chloropyridazin-3(2*H*)-one **5** (2.4 g, 11.5 mmol, 1.0 equiv.) and DIPEA (5.8 mL, 34.5 mmol, 3 equiv.) at 0 °C under nitrogen atmosphere and allowed the reaction

mixture to stir at RT for 16 h. The progress of the reaction was monitored by TLC. The reaction mixture was diluted with ice-cold water (50 mL) and filtered. The resulting solid was washed with water (20 mL) and dried under vacuum to afford (3.0 g, 9.74 mmol, 84%) 1-(6-chloro-3-oxo-2,3-dihydropyridazin-4-yl)-*N*-(furan-2-ylmethyl) azetidine-3-carboxamide **16** as a pale-yellow solid. ^{1}H-NMR (400 MHz, DMSO-d_6): δ 12.46 (s, 1H), 8.49 (t, J = 5.6 Hz, 1H), 7.57–7.54 (m 1H), 6.38 (dd, J = 3.2 Hz, J = 2.0 Hz, 2H), 6.25 (t, J = 0.8 Hz, 1H), 5.92 (s, J = 7.6 Hz, 1H), 4.30–3.90 (m, 4H), 4.49–3.41 (m, 1H); LC-MS (ES-API): m/z = 309.08 $(M + H)^+$, purity by LC-MS: 70%.

*5.2.4.13. Preparation of N-(furan-2-ylmethyl)-1-(3-oxo-6-(pyridin-4-yl)-2,3-dihydropyridazin-4-yl)azetidine-3-carboxamide (**17**).* To a stirred solution of 1-(6-chloro-3-oxo-2,3-dihydropyridazin-4-yl)-*N*-(furan-2-ylmethyl) azetidine-3-carboxamide **16** (200 mg, 0.647 mmol, 1.0 equiv.) in 1,4-dioxane (10 mL) were added 2 N Na_2CO_3 (206 mg, 1.943 mmol, 3.0 equiv.), pyridin-4-yl boronic acid (103.5 mg, 0.842 mmol, 1.3 equiv.) and degassed with argon for 5 minutes before the addition of Pd(dppf)$Cl_2 \cdot CH_2Cl_2$ (53 mg, 0.064 mmol, 0.1 equiv.) was stirred at 100 °C for 16 h. The reaction mixture was diluted with ice-cold water (30 mL) and then extracted with ethyl acetate (EtOAc) (2 × 50 mL). The combined organic layer was washed with brine (20 mL), dried over anhydrous Na_2SO_4, filtered, and concentrated under reduced pressure to afford crude compound, which upon purification by flash chromatography (using Biotage, Claricep, 12 g silica cartridge, eluted with 5–10% of MeOH in CH_2Cl_2) to afford (52 mg, 0/148 mmol, 23%) *N*-(furan-2-ylmethyl)-1-(3-oxo-6-(pyridin-4-yl)-2,3-dihydropyridazin-4-yl)azetidine-3-carboxamide **17** as a light brown solid. ^{1}H-NMR (400 MHz, DMSO-d_6): δ 12.74 (s, 1H), 8.63 (d, J = 5.6 Hz, 2H), 8.50 (t, J = 5.2 Hz, 1H), 7.81 (dd, J = 4.8 Hz, J = 1.2 Hz, 2H), 7.58 (d, J = 2.0 Hz, 1H), 6.51 (s, 1H), 7.39 (dd, J = 3.2 Hz, J = 2.0 Hz, 1H), 6.25 (dd, J = 3.2 Hz, J = 0.4 Hz, 1H), 6.51 (s, 1H), 4.51–4.15 (m, 6H), 3.52–3.45 (m, 1H); ^{13}C-NMR (400 MHz, DMSO-d_6): 171.2, 156.6, 149.9, 145.0, 143.1, 142.1, 120.2, 110.4, 106.8, 98.1, 55.2, 35.5, 33.9; IR: 1653.0 cm^{-1} (C═O stretching); LC-MS (ES-API): m/z = 352.18 $(M + H)^+$; purity by HPLC: 97.9%; MR: 228–230 °C.

*5.2.4.14. Preparation of N-(furan-2-ylmethyl)-1-(3-oxo-6-phenyl-2,3-dihydropyridazin-4-yl)azetidine-3-carboxamide (**18**).* To a stirred solution of 1-(6-chloro-3-oxo-2,3-dihydropyridazin-4-yl)-*N*-(furan-2-ylmethyl) azetidine-3-carboxamide **16** (200 mg, 0.647 mmol, 1.0 equiv.) in 1,4-dioxane (10 mL) were added 2 N Na_2CO_3 (206 mg, 1.943 mmol, 3.0 equiv.), phenylboronic acid (102 mg, 0.842 mmol, 1.3 equiv.) and degassed with argon for 5 minutes before the addition of Pd(dppf)$Cl_2 \cdot CH_2Cl_2$ (53 mg, 0.064 mmol, 0.1 equiv.) was stirred at 100 °C for 16 h. The reaction mixture was diluted with ice-cold water (30 mL) and then extracted with ethyl acetate (EtOAc) (2 × 50 mL). The combined organic layer was washed with brine (20 mL), dried over anhydrous Na_2SO_4, filtered, and concentrated under reduced pressure to afford crude compound, which upon purification by flash chromatography (using Biotage, Claricep, 12 g silica cartridge, eluted with 5–10% of MeOH in CH_2Cl_2) to afford (55 mg, 0.157 mmol, 24%) *N*-(furan-2-ylmethyl)-1-(3-oxo-6-(pyridin-4-yl)-2,3-dihydropyridazin-4-yl)azetidine-3-carboxamide **18** as a pale-yellow solid. ^{1}H-NMR (400 MHz, DMSO-d_6): δ 12.54 (s, 1H), 8.49 (t, J = 5.6 Hz, 1H), 7.81 (d, J = 6.8 Hz, 2H), 7.58 (d, J = 0.8 Hz, 1H), 7.45–7.38 (m, 3H), 6.40–6.38 (m, 2H), 6.25 (d, J = 2.8 Hz, 1H), 4.45–4.23 (m, 6H), 3.51–3.44 (m, 1H); ^{13}C-NMR (400 MHz, DMSO-d_6): 171.2, 156.5, 152.0, 145.4, 145.0, 142.1, 136.1, 128.6, 128.5, 125.7, 110.4, 106.9, 98.9, 55.4, 35.5, 33.9; IR: 1647.2 cm^{-1} (C═O stretching); LC-MS (ES-API): m/z = 351.17 $(M + H)^+$; purity by HPLC: 99.8%; MR: 254–256 °C.

*5.2.4.15. Preparation of 1-(6-(3-fluorophenyl)-3-oxo-2,3-dihydropyridazin-4-yl)-N-(furan-2-ylmethyl)azetidine-3-carboxamide (**19**).* To a stirred solution of 1-(6-chloro-3-oxo-2,3-dihydropyridazin-4-yl)-*N*-(furan-2-ylmethyl) azetidine-3-carboxamide **16** (200 mg, 0.647 mmol, 1.0 equiv.) in 1,4-dioxane (10 mL) were added 2 N Na_2CO_3 (206 mg, 1.943 mmol, 3.0 equiv.), (3-fluorophenyl)boronic acid (117.2 mg, 0.842 mmol, 1.3 equiv.) and degassed with argon for 5 minutes before the addition of Pd(dppf)$Cl_2 \cdot CH_2Cl_2$ (53 mg, 0.064 mmol, 0.1 equiv.) and stirred for 16 h at 100 °C. The reaction mixture was diluted with ice-cold water (30 mL) and then extracted with ethyl acetate (EtOAc) (2 × 50 mL). The combined organic layer was washed with brine (20 mL), dried over anhydrous Na_2SO_4, filtered, and concentrated under reduced pressure to afford crude compound, which, upon purification by flash chromatography (using Biotage, Claricep, 12 g silica cartridge, eluted with 5–10% of MeOH in CH_2Cl_2) to afford (61 mg, 0.165 mmol, 25%) 1-(6-(3-fluorophenyl)-3-oxo-2,3-dihydropyridazin-4-yl)-*N*-(furan-2-ylmethyl)azetidine-3-carboxamide **19** as a pale-yellow solid. ^{1}H-NMR (500 MHz, DMSO-d_6): δ 12.61 (s, 1H), 8.49 (d, J = 6.0 Hz, 1H), 7.69 (d, J = 8.0 Hz, 1H), 7.64 (d, J = 10.0 Hz, 1H), 7.58 (d, J = 1.0 Hz, 1H), 7.49–7.45 (m, 1H), 7.22 (t, J = 10.0 Hz, 1H), 6.45 (s, 1H), 6.39 (d, J = 2.5 Hz, 1H), 6.25 (d, J = 2.5 Hz, 1H), 4.31–4.24 (m, 6H), 3.50–3.46 (m, 1H); ^{13}C-NMR (400 MHz, DMSO-d_6): 171.2, 163.6, 161.2, 156.5, 152.0, 145.0, 144.2, 142.1, 138.6, 138.5, 130.55, 130.47, 121.79, 115.4, 115.2, 112.5, 112.3, 110.4, 106.9, 98.7, 55.3, 35.5, 33.9; IR: 1649.1 cm^{-1} (C═O stretching); LC-MS (ES-API): m/z = 369.19 $(M + H)^+$; purity by HPLC: 99.1%; MR: 263–265 °C.

*5.2.4.16. Preparation of N-(furan-2-ylmethyl)-1-(6-(4-methoxyphenyl)-3-oxo-2,3-dihydropyridazin-4-yl)azetidine-3-carboxamide (**20**).* To a stirred solution of 1-(6-chloro-3-oxo-2,3-dihydropyridazin-4-yl)-*N*-(furan-2-ylmethyl) azetidine-3-carboxamide **16** (200 mg, 0.647 mmol, 1.0 equiv.) in 1,4-dioxane (10 mL) were added 2 N Na_2CO_3 (206 mg, 1.943 mmol, 3.0 equiv), (4-methoxyphenyl)boronic acid (127.9 mg, 0.842 mmol, 1.3 equiv.) and degassed with argon for 5 minutes prior to the addition of Pd(dppf)$Cl_2 \cdot CH_2Cl_2$ (53 mg, 0.064 mmol, 0.1 equiv.) and stirred for 16 h at 100 °C. The reaction mixture was diluted with ice-cold water (30 mL) and then extracted with ethyl acetate (EtOAc) (2 × 50 mL). The combined organic layer was washed with brine (20 mL), dried over anhydrous Na_2SO_4, filtered, and concentrated under reduced pressure to afford crude compound, which upon purification by flash chromatography (using Biotage, Claricep, 12 g silica cartridge, eluted with 5–10% of MeOH in CH_2Cl_2) to afford (55 mg, 0.144 mmol, 22%) *N*-(furan-2-ylmethyl)-1-(6-(4-methoxyphenyl)-3-oxo-2,3-dihydropyridazin-4-yl)azetidine-3-

carboxamide **20** as a light brown solid. ^{1}H-NMR (500 MHz, DMSO-d_6): δ 12.43 (s, 1H), 8.48 (t, J = 6.0 Hz, 1H), 7.75 (d, J = 9.0 Hz, 2H), 7.57 (d, J = 1.0 Hz, 1H), 6.97 (d, J = 9.0 Hz, 2H), 6.39 (d, J = 3.5 Hz, 1H), 6.36 (s, 1H), 6.25 (d, J = 3.5 Hz, 1H), 4.30–4.21 (m, 6H), 3.79 (s, 1H), 3.49–3.45 (m, 1H); ^{13}C-NMR (400 MHz, DMSO-d_6): 171.2, 159.6, 156.4, 152.0, 145.2, 145.0, 142.1, 128.5, 127.0, 113.8, 110.4, 106.9, 98.8, 55.1, 35.5, 34.0; IR: 1649.1 cm^{-1} (C=O stretching); LC-MS (ES-API): m/z = 381.16 (M + H)$^+$; purity by HPLC: 98.4%; MR: 222–225 °C.

*5.2.4.17. Preparation of 1-(6-(4-chlorophenyl)-3-oxo-2,3-dihydropyridazin-4-yl)-N-(furan-2-ylmethyl)azetidine-3-carboxamide (**21**).* To a stirred solution of 1-(6-chloro-3-oxo-2,3-dihydropyridazin-4-yl)-*N*-(furan-2-ylmethyl) azetidine-3-carboxamide **16** (200 mg, 0.647 mmol, 1.0 equiv.) in 1,4-dioxane (10 mL) were added 2 N Na_2CO_3 (206 mg, 1.943 mmol, 3.0 equiv.), (4-chlorophenyl)boronic acid (131 mg, 0.842 mmol, 1.3 equiv.) and degassed with argon for 5 minutes before the addition of Pd(dppf)$Cl_2 \cdot CH_2Cl_2$ (53 mg, 0.064 mmol, 0.1 equiv.) and stirred for 16 h at 100 °C. The reaction mixture was diluted with ice-cold water (30 mL) and then extracted with ethyl acetate (EtOAc) (2 × 50 mL). The combined organic layer was washed with brine (20 mL), dried over anhydrous Na_2SO_4, filtered and concentrated under reduced pressure to afford crude compound, which upon purification by flash chromatography (using Biotage, Claricep, 12 g silica cartridge, eluted with 5–10% of MeOH in CH_2Cl_2) to afford (60 mg, 0.156 mmol, 24%) 1-(6-(4-chlorophenyl)-3-oxo-2,3-dihydropyridazin-4-yl)-*N*-(furan-2-ylmethyl)azetidine-3-carboxamide **21** as a light brown solid. ^{1}H-NMR (500 MHz, DMSO-d_6): δ 12.58 (s, 1H), 8.48 (t, J = 5.5 Hz, 1H), 8.15 (s, 1H), 7.85 (d, J = 6.8 Hz, 2H), 7.57 (d, J = 1.0 Hz, 1H), 7.48 (d, J = 9.0 Hz, 2H), 6.42 (s, 1H), 6.39 (d, J = 3.0 Hz, 1H), 6.25 (d, J = 3.0 Hz, 1H), 4.31–4.21 (m, 6H), 3.79 (s, 1H), 3.50–3.46 (m, 1H); ^{13}C-NMR (400 MHz, DMSO-d_6): 171.2, 156.4, 152.0, 145.0, 144.3, 142.1, 135.9, 135.0, 134.9, 113.3, 131.6, 130.7, 128.5, 127.5, 127.4, 110.4, 106.9, 98.5, 55.5, 35.5, 33.9; IR: 1649.1 cm^{-1} (C=O stretching); LC-MS (ES-API): m/z = 385.1 (M + H)$^+$; purity by HPLC: 73.2%; MR: 241–242 °C.

*5.2.4.18. Preparation of 1-(6-(3,5-difluorophenyl)-3-oxo-2,3-dihydropyridazin-4-yl)-N-(furan-2-ylmethyl)azetidine-3-carboxamide (**22**).* To a stirred solution of 1-(6-chloro-3-oxo-2,3-dihydropyridazin-4-yl)-*N*-(furan-2-ylmethyl) azetidine-3-carboxamide **16** (200 mg, 0.647 mmol, 1.0 equiv.) in 1,4-dioxane (10 mL) were added 2 N Na_2CO_3 (206 mg, 1.943 mmol, 3.0 equiv.), (3,5-difluorophenyl)boronic acid (132.9 mg, 0.842 mmol, 1.3 equiv.) and degassed with argon for 5 minutes prior to the addition of Pd(dppf)$Cl_2 \cdot CH_2Cl_2$ (53 mg, 0.064 mmol, 0.1 equiv.) and stirred for 16 h at 100 °C. The reaction mixture was diluted with ice-cold water (30 mL) and then extracted with ethyl acetate (EtOAc) (2 × 50 mL). The combined organic layer was washed with brine (20 mL), dried over anhydrous Na_2SO_4, filtered, and concentrated under reduced pressure to afford crude compound, which upon purification by flash chromatography (using Biotage, Claricep, 12 g silica cartridge, eluted with 5–10% of MeOH in CH_2Cl_2) to afford (58 mg, 0.15 mmol, 23%) 1-(6-(3,5-difluorophenyl)-3-oxo-2,3-dihydropyridazin-4-yl)-*N*-(furan-2-ylmethyl)azetidine-3-carboxamide **22** as a light brown solid. ^{1}H-NMR (400 MHz, DMSO-d_6): δ 12.66 (s, 1H), 8.48 (d, J = 5.6 Hz, 1H), 7.69–7.63 (m, 1H), 7.57 (d, J = 1.6 Hz, 1H), 7.35 (t, J = 9.2 Hz, 1H), 7.17 (t, J = 8.4 Hz, 1H), 6.38 (d, J = 3.2 Hz, 1H), 6.24 (d, J = 2.8 Hz, 1H), 6.13 (d, J = 1.6 Hz, 1H), 4.30–4.18 (m, 6H), 3.50–3.45 (m, 1H); ^{13}C-NMR (400 MHz, DMSO-d_6): 171.2, 163.6, 163.4, 161.1, 161.0, 160.8, 160.2, 158.3, 158.2, 156.3, 151.9, 144.6, 142.1, 142.0, 131.4, 131.3, 130.6, 128.5, 121.4, 121.3, 111.9, 111.7, 110.4, 106.9, 104.5, 104.2, 101.4, 101.3, 54.9, 35.5, 33.9; IR: 1651.1 cm^{-1} (C=O stretching); LC-MS (ES-API): m/z = 387.13 (M + H)$^+$; purity by HPLC: 97.3%; MR: 215–218 °C.

*5.2.4.19. Preparation of methyl 5-(5-(3-((furan-2-ylmethyl) carbamoyl)azetidin-1-yl)-6-oxo-1,6-dihydropyridazin-3-yl) nicotinate (**23**).* To a stirred solution of 1-(6-chloro-3-oxo-2,3-dihydropyridazin-4-yl)-*N*-(furan-2-ylmethyl) azetidine-3-carboxamide **16** (200 mg, 0.647 mmol, 1.0 equiv.) in 1,4-dioxane (10 mL) were added 2 N Na_2CO_3 (206 mg, 1.943 mmol, 3.0 equiv.), (5-(methoxycarbonyl)pyridin-3-yl)boronic acid (152.3 mg, 0.842 mmol, 1.3 equiv.) and degassed with argon for 5 minutes before the addition of Pd(dppf)$Cl_2 \cdot CH_2Cl_2$ (53 mg, 0.064 mmol, 0.1 equiv.) and stirred for 16 h at 100 °C. The reaction mixture was diluted with ice-cold water (30 mL) and then extracted with ethyl acetate (EtOAc) (2 × 50 mL). The combined organic layer was washed with brine (20 mL), dried over anhydrous Na_2SO_4, filtered, and concentrated under reduced pressure to afford crude compound, which, upon purification by flash chromatography (using Biotage, Claricep, 12 g silica cartridge, eluted with 5–10% of MeOH in CH_2Cl_2) to afford (65 mg, 0.158 mmol, 25%) methyl 5-(5-(3-((furan-2-ylmethyl)carbamoyl)azetidin-1-yl)-6-oxo-1,6-dihydropyridazin-3-yl)nicotinate **23** as a light brown solid. ^{1}H-NMR (400 MHz, DMSO-d_6): δ 12.74 (s, 1H), 9.26 (t, J = 2.0 Hz, 1H), 9.08 (d, J = 2.0 Hz, 1H), 8.65 (d, J = 2.0 Hz, 1H), 8.50 (d, J = 5.6 Hz, 1H), 7.58 (d, J = 1.2 Hz, 1H), 6.59 (s, 1H), 6.39 (d, J = 2.4 Hz, 1H), 6.25 (d, J = 2.4 Hz, 1H), 4.51–4.32 (m, 6H), 3.92 (s, 1H), 3.52–3.48 (m, 1H); ^{13}C-NMR (400 MHz, DMSO-d_6): 171.2, 165.0, 156.4, 152.0, 150.6, 149.6, 145.1, 142.2, 142.1, 133.3, 131.9, 130.6, 128.5, 125.4, 110.4, 106.9, 98.2, 55.8, 35.5, 33.9; IR: 1649.1 cm^{-1} (C=O stretching); LC-MS (ES-API): m/z = 410.14 (M + H)$^+$; purity by HPLC: 92.9%; MR: 257–260 °C.

*5.2.4.20. Preparation of tert-butyl 3-(4-phenylpiperazine-1-carbonyl)azetidine-1-carboxylate (**25**).* To a stirred solution of 1-(*tert*-butoxycarbonyl)azetidine-3-carboxylic acid **1** (3 g, 14.909 mmol, 1 equiv.) in DMF (20 mL) at 0 °C under nitrogen atmosphere were added DIPEA (7.69 mL, 44.727 mmol, 3 equiv.), HATU (7.6 g, 19.38 mmol, 1.3 equiv.) and 1-phenylpiperazine **24** (2.66 g, 16.399 mmol, 1.1 equiv.). The resulting reaction mixture was stirred at RT for 16 h. The progress of the reaction was monitored by TLC. The reaction mixture was diluted with water (50 mL) and extracted with EtOAc (2 × 100 mL). The combined organic layer was washed with brine (2 × 30 mL), dried over anhydrous sodium sulphate, filtered and concentrated under reduced pressure to get the crude product, which upon purification by flash chromatography (using Biotage, Claricep, 80 g silica cartridge, eluted with 35–40% of EtOAc in petether) to afford (3.4 g, 9.85 mmol, 66%) *tert*-butyl 3-(4-phenylpiperazine-1-carbonyl)azetidine-1-carboxylate **25** as a pale-yellow solid. ^{1}H-NMR (400 MHz, $CDCl_3$): δ 7.30–7.26 (m,

2H), 6.93–6.90 (m, 3H), 4.20–4.06 (m, 4H), 3.79 (t, J = 4.8 Hz, 2H), 3.52–3.41 (m, 3H), 3.17–3.13 (m, 4H), 1.43 (s, 9H); LC-MS (ES-API): m/z = 346.7 $(M + H)^+$, purity by LC-MS: 86.5%.

*5.2.4.21. Preparation of azetidin-3-yl(4-phenylpiperazin-1-yl) methanone (**26**).* To a stirred solution of *tert*-butyl 3-((furan-2-ylmethyl)carbamoyl)azetidine-1-carboxylate **25** (3.4 g, 9.85 mmol, 1 equiv.) in CH_2Cl_2 (35 mL) was added TFA (3.8 mL, 49.21 mmol, 5.0 equiv.) at 0 °C. The resulting reaction mixture was stirred at RT for 2 h. The progress of the reaction was monitored by TLC and LC-MS. After completion of the reaction, the reaction mixture was concentrated under reduced pressure, and the residue was triturated with diethyl ether (30 mL) and dried under vacuum to get (3.2 g, 9.32 mmol, 94%) of azetidine-3-yl (4-phenylpiperazin-1-yl)methanone (**26**) (TFA salt) as a pale-yellow solid. LC-MS (ES-API): m/z = 246.56 $(M + H)^+$, purity by LC-MS (crude): 44.3%.

*5.2.4.22. Preparation of 6-chloro-4-(3-(4-phenylpiperazine-1-carbonyl)azetidin-1-yl)pyridazin-3(2H)-one (**27**).* To a stirred solution of azetidin-3-yl(4-phenylpiperazin-1-yl)methanone **26** (TFA salt) (3.2 g, 9.32 mmol, 1.0 equiv.) in DMF (30 mL) were added 4-bromo-6-chloropyridazin-3(2*H*)-one **5** (1.95g, 9.32 mmol, 1.0 equiv.) and DIPEA (4.8 mL, 27.96 mmol, 3 equiv.) at 0 °C under nitrogen atmosphere and allowed the reaction mixture to stir at RT for 16 h. The progress of the reaction was monitored by TLC. The reaction mixture was diluted with ice-cold water (50 mL) and filtered the resulting solid, washed with water (20 mL), and dried under vacuum to afford (3.0 g, 8.04 mmol. 86%) 6-chloro-4-(3-(4-phenylpiperazine-1-carbonyl) azetidin-1-yl)pyridazin-3(2*H*)-one **27** as a pale-yellow solid. ^{1}H-NMR (400 MHz, $CDCl_3$): δ 9.85 (s, 1H), 7.31–7.26 (m, 2H), 6.94–6.89 (m, 3H), 5.74 (s, 1H), 4.57–4.46 (m, 4H), 3.82–3.73 (m, 4H), 3.48–3.43 (m, 3H), 3.21–3.17 (m, 2H); LC-MS (ES-API): m/z = 374.05 $(M + H)^+$, purity by LC-MS: 78.9%.

*5.2.4.23. Preparation of 4-(3-(4-phenylpiperazine-1-carbonyl) azetidin-1-yl)-6-(pyridin-4-yl)pyridazin-3(2H)-one (**28**).* To a stirred solution of 6-chloro-4-(3-(4-phenylpiperazine-1-carbonyl)azetidin-1-yl)pyridazin-3(2*H*)-one **27** (200 mg, 0.534 mmol, 1.0 equiv.) in 1,4-dioxane (10 mL) were added 2 N Na_2CO_3 (170 mg, 1.604 mmol, 3.0 equiv.), pyridin-4-yl boronic acid (85 mg, 0.694 mmol, 1.3 equiv.) and degassed with argon for 5 minutes before the addition of $Pd(dppf)Cl_2 \cdot CH_2Cl_2$ (43 mg, 0.053 mmol, 0.1 equiv.) and stirred for 16 h at 100 °C. The reaction mixture was diluted with ice-cold water (30 mL) and extracted with EtOAc (2 × 50 mL). The combined organic layer was washed with brine (20 mL), dried over anhydrous Na_2SO_4, filtered and concentrated under reduced pressure to afford crude compound, which upon purification by flash chromatography (using Biotage, Claricep, 12 g silica cartridge, eluted with 5–10% of MeOH in CH_2Cl_2) to afford (35 mg, 0.084 mmol, 16%) 4-(3-(4-phenylpiperazine-1-carbonyl)azetidin-1-yl)-6-(pyridin-4-yl)pyridazin-3(2*H*)-one **28** as a as a light brown solid. ^{1}H-NMR (400 MHz, DMSO-d_6): δ 12.77 (s, 1H), 8.63 (d, J = 5.6 Hz, 2H), 7.81 (dd, J = 4.8 Hz, J = 1.6 Hz, 2H), 7.23 (t, J = 8.4 Hz, 2H), 6.97 (d, J = 8.0 Hz, 2H), 6.81 (t, J = 8.0 Hz, 1H), 6.55 (s, 1H), 4.59–4.19 (m, 4H), 3.91–3.88 (m, 1H), 3.64 (t, J = 4.4 Hz, 2H), 3.46 (t, J = 4.4 Hz, 2H), 3.17–3.14 (m, 4H); ^{13}C-NMR (400 MHz, DMSO-d_6): 169.3, 156.6, 150.7, 150.0, 145.1, 143.1, 128.1, 119.9, 119.3, 115.9, 98.3, 48.6, 48.2, 44.3, 32.1; IR: 1656.8 cm^{-1} (C=O stretching); LC-MS (ES-API): m/z = 417.29 $(M + H)^+$; purity by HPLC: 97.8%; MR: 261–263 °C.

*5.2.4.24. Preparation of 6-phenyl-4-(3-(4-phenylpiperazine-1-carbonyl)azetidin-1-yl)pyridazin-3(2H)-one (**29**).* To a stirred solution of 6-chloro-4-(3-(4-phenylpiperazine-1-carbonyl)azetidin-1-yl)pyridazin-3(2*H*)-one **27** (200 mg, 0.534 mmol, 1.0 equiv.) in 1,4-dioxane (10 mL) were added 2 N Na_2CO_3 (170 mg, 1.604 mmol, 3.0 equiv.), phenylboronic acid (84 mg, 0.694 mmol, 1.3 equiv.) and degassed with argon for 5 minutes before the addition of $Pd(dppf)Cl_2 \cdot CH_2Cl_2$ (43 mg, 0.053 mmol, 0.1 equiv.) and stirred for 16 h at 100 °C. The reaction mixture was diluted with ice-cold water (30 mL) and extracted with EtOAc (2 × 50 mL). The combined organic layer was washed with brine (20 mL), dried over anhydrous Na_2SO_4, filtered, and concentrated under reduced pressure to afford crude compound, which, upon purification by flash chromatography (using Biotage, Claricep, 12 g silica cartridge, eluted with 5–10% of MeOH in CH_2Cl_2) to afford (40 mg, 0.096 mmol, 18%) 6-phenyl-4-(3-(4-phenylpiperazine-1-carbonyl)azetidin-1-yl)pyridazin-3(2*H*)-one **29** as a light brown solid. ^{1}H-NMR (400 MHz, DMSO-d_6): δ 12.56 (s, 1H), 7.82 (d, J = 6.8 Hz, 2H), 7.45–7.38 (m, 3H), 7.23 (t, J = 8.0 Hz, 2H), 6.97 (d, J = 8.0 Hz, 2H), 6.81 (t, J = 7.2 Hz, 1H), 6.45 (s, 1H),4.51–4.29 (m, 4H), 3.91–3.88 (m, 1H), 3.71–3.60 (m, 2H), 3.50–3.40 (m, 2H), 3.17–3.14 (m, 4H); ^{13}C-NMR (400 MHz, DMSO-d_6): 169.3, 156.5, 150.7, 145.4, 145.1, 136.0, 128.9, 128.6, 128.5, 125.7, 119.3, 115.9, 99.0, 48.6, 48.2, 44.3, 32.0; IR: 1647.2 cm^{-1} (C=O stretching); LC-MS (ES-API): m/z = 416.25 $(M + H)^+$; purity by HPLC: 98.9%; MR: 239–242 °C.

*5.2.4.25. Preparation of tert-butyl 3-((2,2,2-trifluoroethyl) carbamoyl)azetidine-1-carboxylate (**31**).* To a stirred solution of 1-(*tert*-butoxycarbonyl)azetidine-3-carboxylic acid (**1**) (3 g, 14.909 mmol, 1 equiv.) in DMF (20 mL) at 0 °C under nitrogen atmosphere were added DIPEA (7.69 mL, 44.727 mmol, 3 equiv.), HATU (7.6 g, 19.38 mmol, 1.3 equiv.) and 2,2,2-trifluoroethan-1-amine **30** (1.62 g, 16.399 mmol, 1.1 equiv.). The resulting reaction mixture was stirred at RT for 16 h. The progress of the reaction was monitored by TLC. The reaction mixture was diluted with water (50 mL) and extracted with EtOAc (2 × 100 mL). The combined organic layer was washed with brine (2 × 30 mL), dried over anhydrous sodium sulphate, filtered and concentrated under reduced pressure to get the crude product, which upon purification by flash chromatography (using Biotage, Claricep, 80 g silica cartridge, eluted with 35–40% of EtOAc in petether) to afford (3.4 g, 12.01 mmol, 81%) *tert*-butyl 3-((2,2,2-trifluoroethyl)carbamoyl)azetidine-1-carboxylate **31** as a pale-yellow solid. ^{1}H-NMR (400 MHz, $CDCl_3$): δ 6.02 (s, 1H), 4.13–4.05 (m, 4H), 3.99–3.91 (m, 2H), 3.28–3.21 (m, 1H), 1.43 (s, 9H); LC-MS (ES-API): m/z = 283.12 $(M + H)^+$, purity by LC-MS: 99.7%.

*5.2.4.26. Preparation of N-(2,2,2-trifluoroethyl)azetidine-3-carboxamide (**32**).* To a solution of *tert*-butyl 3-((furan-2-ylmethyl)carbamoyl)azetidine-1-carboxylate **31** (3.4 g, 12.04 mmol, 1 equiv.) in CH_2Cl_2 (35 mL) was added TFA (4.6 mL, 60.22 mmol, 5.0 equiv.) at 0 °C. The resulting reaction mixture was stirred at RT for 2 h. The progress of the reaction was monitored by TLC and LC-MS. After completion of the reaction,

the reaction mixture was concentrated under reduced pressure, and the residue was triturated with diethyl ether (30 mL), and dried under vacuum to get (3.2 g, 11.42 mmol, 95%) *N*-(2,2,2-trifluoromethyl)azetidine-3-carboxamide **32** (TFA salt) as a pale-yellow solid. LC-MS (ES-API): $m/z = 183.09$ $(M + H)^+$, purity by LC-MS: 99%.

*5.2.4.27. Preparation of 1-(6-chloro-3-oxo-2,3-dihydropyridazin-4-yl)-N-(2,2,2-trifluoroethyl)azetidine-3-carboxamide (**33**).* To a stirred solution of *N*-(2,2,2-trifluoroethyl) azetidine-3-carboxamide **32** (3.2 g, 11.42 mmol, 1.0 equiv.) in DMF (30 mL) were added 4-bromo-6-chloropyridazin-3(2*H*)-one **5** (2.38 g, 11.42 mmol, 1.0 equiv.) and DIPEA (5.8 mL, 34.26 mmol, 3 equiv.) at 0 °C under nitrogen atmosphere and allowed the reaction mixture to stir at RT for 16 h. The progress of the reaction was monitored by TLC. The reaction mixture was diluted with ice-cold water (50 mL) and filtered the resulting solid, washed with water (20 mL), and dried under vacuum to afford (3.1 g, 10.0 mmol, 87%) 1-(6-chloro-3-oxo-2,3-dihydropyridazin-4-yl)-*N*-(2,2,2-trifluoroethyl)azetidine-3-carboxamide **33** as a pale-yellow solid. ^{1}H-NMR (400 MHz, DMSO-d_6): δ 12.48 (s, 1H), 8.70 (t, $J = 6.4$ Hz, 1H), 7.45–7.38 (m, 3H), 5.94 (s, 1H),4.46–3.82 (m, 6H), 3.57–3.46 (m, 1H); LC-MS (ES-API): $m/z = 311.05$ $(M + H)^+$, purity by LC-MS: 81%.

*5.2.4.28. Preparation of 1-(3-oxo-6-(pyridin-4-yl)-2,3-dihydropyridazin-4-yl)-N-(2,2,2-trifluoroethyl)azetidine-3-carboxamide (**34**).* To a stirred solution of 1-(6-chloro-3-oxo-2,3-dihydropyridazin-4-yl)-*N*-(2,2,2-trifluoroethyl)azetidine-3-carboxamide **33** (200 mg, 0.643 mmol, 1.0 equiv.) in 1,4-dioxane (10 mL) were added 2 N Na_2CO_3 (204 mg, 1.931 mmol, 3.0 equiv.), pyridin-4-yl boronic acid (102 mg, 0.835 mmol, 1.3 equiv.) and degassed with argon for 5 minutes prior to the addition of Pd(dppf)$Cl_2 \cdot CH_2Cl_2$ (52 mg, 0.064 mmol, 0.1 equiv.) and stirred for 16 h at 100 °C. The reaction mixture was diluted with ice-cold water (30 mL) and extracted with EtOAc (2 × 50 mL). The combined organic layer was washed with brine (20 mL), dried over anhydrous Na_2SO_4, filtered, and concentrated under reduced pressure to afford crude compound, which, upon purification by flash chromatography (using Biotage, Claricep, 12 g silica cartridge, eluted with 5–10% of MeOH in CH_2Cl_2) to afford (65 mg, 0.184 mmol, 28%) 1-(3-oxo-6-(pyridin-4-yl)-2,3-dihydropyridazin-4-yl)-*N*-(2,2,2-trifluoroethyl)azetidine-3-carboxamide **34** as a light brown solid. ^{1}H-NMR (400 MHz, DMSO-d_6): δ 12.76 (s, 1H), 8.71 (t, $J = 6.0$ Hz, 1H), 8.63 (br s, 2H), 7.82 (d, $J = 5.2$ Hz, 2H), 6.53 (s, 1H), 4.45–4.21 (m, 4H), 4.01–3.91 (m, 2H), 3.56–3.53 (m, 1H); ^{13}C-NMR (400 MHz, DMSO-d_6): 171.3, 156.6, 150.7, 145.0, 143.1, 128.8, 126.1, 123.3, 120.0, 98.3, 55.3, 33.9; IR: 1658.7 cm^{-1} (C=O stretching); LC-MS (ES-API): $m/z = 354.14$ $(M + H)^+$; purity by HPLC: 99.3%; MR: 273–276 °C.

*5.2.4.29. Preparation of 1-(3-oxo-6-phenyl-2,3-dihydropyridazin-4-yl)-N-(2,2,2-trifluoroethyl)azetidine-3-carboxamide (**35**).* To a stirred solution of 1-(6-chloro-3-oxo-2,3-dihydropyridazin-4-yl)-*N*-(2,2,2-trifluoroethyl)azetidine-3-carboxamide **33** (200 mg, 0.643 mmol, 1.0 equiv.) in 1,4-dioxane (10 mL) were added 2 N Na_2CO_3 (204 mg, 1.931 mmol, 3.0 equiv.), phenylboronic acid (102 mg, 0.835 mmol, 1.3 equiv.) and degassed with argon for 5 minutes prior to the addition of Pd(dppf)$Cl_2 \cdot CH_2Cl_2$ (52 mg, 0.064 mmol, 0.1 equiv.) and stirred for 16 h at 100 °C. The reaction mixture was diluted with ice-cold water (30 mL) and extracted with EtOAc (2 × 50 mL). The combined organic layer was washed with brine (20 mL), dried over anhydrous Na_2SO_4, filtered, and concentrated under reduced pressure to afford crude compound, which upon purification by flash chromatography (using Biotage, Claricep, 12 g silica cartridge, eluted with 5–10% of MeOH in CH_2Cl_2) to afford (60 mg, 0.17 mmol, 25%) 1-(3-oxo-6-phenyl-2,3-dihydropyridazin-4-yl)-*N*-(2,2,2-trifluoroethyl)azetidine-3-carboxamide **35** as a light brown solid. ^{1}H-NMR (400 MHz, DMSO-d_6): δ 12.56 (s, 1H), 8.71 (t, $J = 6.4$ Hz, 1H), 7.83 (t, $J = 7.2$ Hz, 2H), 7.45–7.37 (m, 3H), 6.43 (s, 1H), 4.45–4.21 (m, 4H), 4.01–3.91 (m, 2H), 3.57–3.50 (m, 1H); ^{13}C-NMR (400 MHz, DMSO-d_6): 172.3, 156.5, 145.4, 145.0, 136.1, 128.6, 128.5, 126.1, 125.7, 123.3, 99.0, 55.3, 54.8, 33.9; IR: 1658.7 cm^{-1} (C=O stretching); LC-MS (ES-API): $m/z = 353.17$ $(M + H)^+$; purity by HPLC: 97.7%; MR: 237–239 °C.

*5.2.4.30. Preparation of 1-(6-(3-fluorophenyl)-3-oxo-2,3-dihydropyridazin-4-yl)-N-(2,2,2-trifluoroethyl)azetidine-3-carboxamide (**36**).* To a stirred solution of 1-(6-chloro-3-oxo-2,3-dihydropyridazin-4-yl)-*N*-(2,2,2-trifluoroethyl)azetidine-3-carboxamide **33** (200 mg, 0.643 mmol, 1.0 equiv.) in 1,4-dioxane (10 mL) were added 2 N Na_2CO_3 (204 mg, 1.931 mmol, 3.0 equiv.), (3-fluorophenyl)boronic acid (116.8 mg, 0.835 mmol, 1.3 equiv.) and degassed with argon for 5 minutes prior to the addition of Pd(dppf)$Cl_2 \cdot CH_2Cl_2$ (52 mg, 0.064 mmol, 0.1 equiv.) and stirred for 16 h at 100 °C. The reaction mixture was diluted with ice-cold water (30 mL) and extracted with EtOAc (2 × 50 mL). The combined organic layer was washed with brine (20 mL), dried over anhydrous Na_2SO_4, filtered, and concentrated under reduced pressure to afford crude compound, which, upon purification by flash chromatography using Biotage, Claricep, 12 g silica cartridge, eluted with 5–10% of MeOH in CH_2Cl_2 to afford (65 mg, 0.175 mmol, 28%) 1-(6-(3-fluorophenyl)-3-oxo-2,3-dihydropyridazin-4-yl)-*N*-(2,2,2-trifluoroethyl) azetidine-3-carboxamide **36** as a light brown solid. ^{1}H-NMR (400 MHz, DMSO-d_6): δ 12.62 (s, 1H), 8.71 (t, $J = 6.0$ Hz, 1H), 7.70–7.63 (m, 2H), 7.50–7.44 (m, 1H), 7.24–7.20 (m, 1H), 6.47 (s, 1H), 4.45–4.24 (m, 4H), 4.01–3.91 (m, 2H), 3.57–3.50 (m, 1H); ^{13}C-NMR (400 MHz, DMSO-d_6): 172.3, 163.6, 161.2, 156.5, 145.0, 144.2, 138.6, 138.5, 130.5, 130.4, 128.8, 126.1, 123.3, 121.7, 120.5, 115.4, 115.2, 112.5, 112.3, 98.8, 55.1, 33.9; IR: 1678.0 cm^{-1} (C=O stretching); LC-MS (ES-API): $m/z = 371.10$ $(M + H)^+$; purity by HPLC: 99.5%; MR: 266–269 °C.

*5.2.4.31. Preparation of 1-(6-(4-methoxyphenyl)-3-oxo-2,3-dihydropyridazin-4-yl)-N-(2,2,2-trifluoroethyl)azetidine-3-carboxamide (**37**).* To a stirred solution of 1-(6-chloro-3-oxo-2,3-dihydropyridazin-4-yl)-*N*-(2,2,2-trifluoroethyl)azetidine-3-carboxamide **33** (200 mg, 0.643 mmol, 1.0 equiv.) in 1,4-dioxane (10 mL) were added 2 N Na_2CO_3 (204 mg, 1.931 mmol, 3.0 equiv.), (4-methoxyphenyl)boronic acid (126.8 mg, 0.835 mmol, 1.3 equiv.) and degassed with argon for 5 minutes before the addition of Pd(dppf)$Cl_2 \cdot CH_2Cl_2$ (52 mg, 0.064 mmol, 0.1 equiv.) and stirred for 16 h at 100 °C. The reaction mixture was diluted with ice-cold water (30 mL) and extracted with EtOAc (2 × 50 mL). The combined organic layer was washed with brine (20 mL), dried over anhydrous Na_2SO_4, filtered, and concentrated

under reduced pressure to afford crude compound, which, upon purification by flash chromatography (using Biotage, Claricep, 12 g silica cartridge, eluted with 5–10% of MeOH in CH_2Cl_2) to afford (60 mg, 0.136 mmol, 25%) 1-(6-(4-methoxyphenyl)-3-oxo-2,3-dihydropyridazin-4-yl)-*N*-(2,2,2-trifluoroethyl) azetidine-3-carboxamide **37** as a light brown solid. ^{1}H-NMR (400 MHz, DMSO-d_6): δ 12.46 (s, 1H), 8.71 (t, J = 6.4 Hz, 1H), 7.75 (d, J = 6.8 Hz, 2H), 6.97 (d, J = 8.8 Hz, 2H), 6.38 (s, 1H), 4.39–4.21 (m, 4H), 3.99–3.91 (m, 2H), 3.79 (s, 3H), 3.55–3.51 (m, 1H); ^{13}C-NMR (400 MHz, DMSO-d_6): 172.3, 159.7, 156.4, 145.2, 145.0, 130.7, 130.61, 128.8, 128.5, 127.1, 126.1, 123.3, 113.8, 98.9, 55.1, 33.9; IR: 1656.5 cm^{-1} (C=O stretching); LC-MS (ES-API): m/z = 383.11 $(M + H)^+$; purity by HPLC: 97.9%; MR: 241–243 °C.

*5.2.4.32. Preparation of 1-(6-(4-chlorophenyl)-3-oxo-2,3-dihydropyridazin-4-yl)-N-(2,2,2-trifluoroethyl)azetidine-3-carboxamide (**38**).* To a stirred solution of 1-(6-chloro-3-oxo-2,3-dihydropyridazin-4-yl)-*N*-(2,2,2-trifluoroethyl)azetidine-3-carboxamide **33** (200 mg, 0.643 mmol, 1.0 equiv.) in 1,4-dioxane (10 mL) were added 2 N Na_2CO_3 (204 mg, 1.931 mmol, 3.0 equiv), (4-chlorophenyl)boronic acid (130.56 mg, 0.835 mmol, 1.3 equiv.) and degassed with argon for 5 minutes prior to the addition of Pd(dppf)$Cl_2 \cdot CH_2Cl_2$ (52 mg, 0.064 mmol, 0.1 equiv.) and stirred for 16 h at 100 °C. The reaction mixture was diluted with ice-cold water (30 mL) and extracted with EtOAc (2 × 50 mL). The combined organic layer was washed with brine (20 mL), dried over anhydrous Na_2SO_4, filtered and concentrated under reduced pressure to afford crude compound, which upon purification by flash chromatography (using Biotage, Claricep, 12 g silica cartridge, eluted with 5–10% of MeOH in CH_2Cl_2) to afford (55 mg, 22%) 1-(6-(4-chlorophenyl)-3-oxo-2,3-dihydropyridazin-4-yl)-*N*-(2,2,2-trifluoroethyl)azetidine-3-carboxamide **38** as a light brown solid. ^{1}H-NMR (400 MHz, DMSO-d_6): δ 12.60 (s, 1H), 8.70 (t, J = 5.2 Hz, 1H), 7.86 (d, J = 6.8 Hz, 2H), 7.49 (d, J = 6.8 Hz, 2H), 6.44 (s, 1H), 4.39–4.21 (m, 4H), 3.99–3.92 (m, 2H), 3.55–3.52 (m, 1H); ^{13}C-NMR (400 MHz, DMSO-d_6): 172.3, 156.4, 145.0, 144.3, 135.9, 134.9, 133.3, 130.7, 128.9, 128.5, 127.5, 126.1, 123.3, 120.5, 99.7, 55.2, 33.9; IR: 1662.6 cm^{-1} (C=O stretching); LC-MS (ES-API): m/z = 387.09 $(M + H)^+$; purity by HPLC: 90.9%; MR: 263–265 °C.

*5.2.4.33. Preparation of 1-(6-(2,4-difluorophenyl)-3-oxo-2,3-dihydropyridazin-4-yl)-N-(2,2,2-trifluoroethyl)azetidine-3-carboxamide (**39**).* To a stirred solution of 1-(6-chloro-3-oxo-2,3-dihydropyridazin-4-yl)-*N*-(2,2,2-trifluoroethyl)azetidine-3-carboxamide **33** (200 mg, 0.643 mmol, 1.0 equiv.) in 1,4-dioxane (10 mL) were added 2 N Na_2CO_3 (204 mg, 1.931 mmol, 3.0 equiv.), (3,5-difluorophenyl)boronic acid (205.2 mg, 0.835 mmol, 1.3 equiv.) and degassed with argon for 5 minutes before the addition of Pd(dppf)$Cl_2 \cdot CH_2Cl_2$ (52 mg, 0.064 mmol, 0.1 equiv.) and stirred for 16 h at 100 °C. The reaction mixture was diluted with ice-cold water (30 mL) and extracted with EtOAc (2 × 50 mL). The combined organic layer was washed with brine (20 mL), dried over anhydrous Na_2SO_4, filtered and concentrated under reduced pressure to afford crude compound, which upon purification by flash chromatography (using Biotage, Claricep, 12 g silica cartridge, eluted with 5–10% of MeOH in CH_2Cl_2) to afford (60 mg, 0.154 mmol, 26%) 1-(6-(2,4-difluorophenyl)-3-oxo-2,3-dihydropyridazin-4-yl)-*N*-(2,2,2-trifluoroethyl)azetidine-3-carboxamide **39** as a light brown solid. ^{1}H-NMR (400 MHz, DMSO-d_6): δ 12.68 (s, 1H), 8.71 (t, J = 6.4 Hz, 1H), 7.69–7.63 (m, 1H), 7.19–7.14 (m, 1H), 6.15 (t, J = 2.0 Hz, 1H), 4.39–4.15 (m, 4H), 3.99–3.90 (m, 2H), 3.56–3.49 (m, 1H); ^{13}C-NMR (400 MHz, DMSO-d_6): 172.3, 163.6, 163.5, 161.1, 161.0, 160.8, 160.7, 158.3, 158.2, 156.3, 144.6, 142.0, 131.4, 128.8, 126.0, 123.3, 121.3, 111.9, 111.7, 104.8, 104.5, 104.2, 101.6, 101.5, 55.2, 33.9; IR: 1645.2 cm^{-1} (C=O stretching); LC-MS (ES-API): m/z = 389.12 $(M + H)^+$; purity by HPLC: 91.2%; MR: 268–271 °C.

*5.2.4.34. Preparation of tert-butyl 3-(2-tosylhydrazineylidene) azetidine-1-carboxylate (**41**).*[19] To a stirred solution of *tert*-butyl 3-oxoazetidine-1-carboxylate **40** (500 mg, 2.92 mmol) in toluene (5 mL) was added tosyl hydrazine (543 mg, 2.92 mmol) at RT. The resulting reaction mixture was stirred at 110 °C for 30 min. The reaction mixture was cooled, filtered, and the solid was washed with petroleum ether (5 mL) to get *tert*-butyl 3-(2-tosylhydrazineylidene)azetidine-1-carboxylate **41** (510 mg, 52%) as an off-white solid; LC-MS (ES-API): m/z = 338.3 $(M–H)^+$.

*5.2.4.35. Preparation of tert-butyl 3-isonicotinoylazetidine-1-carboxylate (**43**).*[20] To a stirred solution of *tert*-butyl 3-(2-tosylhydrazineylidene)azetidine-1-carboxylate **41** (633 mg, 1.86 mmol) and pyridine-4-carbaldehyde **42** (200 mg, 1.86 mmol) in 1,4-dioxane (10 mL) at RT was added Cs_2CO_3 (906 mg, 2.80 mmol). The resulting reaction mixture was stirred at 100 °C for 1 h using a sealed tube and monitored by TLC and LC-MS. After the reaction was completed, the reaction mixture was cooled, diluted with water (5 mL), and extracted with ethyl acetate (3 × 20 mL). The separated organic layer was washed with water and brine, dried over sodium sulfate, filtered, and concentrated under reduced pressure to afford the crude product. This was purified by Grace using 12 g of silica (REVELERIS) eluted with 30–35% ethyl acetate in pet-ether to yield 200 mg (0.763 mmol, 41%) of *tert*-butyl 3-isonicotinoylazetidine-1-carboxylate **43**, as a pale-yellow liquid. ^{1}H-NMR (400 MHz, $CDCl_3$): δ 8.84 (dd, J = 4.8 Hz, J = 1.6 Hz, 2H), 7.62 (dd, J = 4.8 Hz, J = 1.6 Hz, 2H), 4.22 (d, J = 7.2 Hz, 4H), 4.15–4.09 (m, 1H), 1.44 (s, 9H); LC-MS (ES-API): m/z = 263.1 $(M + H)^+$, purity by LC-MS: 92.1%.

*5.2.4.36. Preparation of azetidin-3-yl(pyridin-4-yl)methanone (**44**).* To a stirred solution of *tert*-butyl 3-isonicotinoylazetidine-1-carboxylate **43** (100 mg, 0.381 mmol) in CH_2Cl_2 (1 mL) was added TFA (0.2 mL). The resulting reaction mixture was stirred at RT for 1 h. After completion of the reaction, the reaction mixture was concentrated to afford crude products (64 mg, 0.39 mmol, 64%) azetidin-3-yl(pyridin-4-yl) methanone **44** (TFA salt) as a pale-yellow solid; LC-MS (ES-API): m/z = 163.1 $(M + H)^+$, purity by LC-MS: 94%.

*5.2.4.36. Preparation of 6-chloro-4-(3-isonicotinoylazetidin-1-yl)pyridazin-3(2H)-one (**45**).* To a stirred solution of 4-bromo-6-chloropyridazin-3(2*H*)-one **5** (100 mg, 0.478 mmol) and azetidin-3-yl(pyridin-4-yl)methanone **44** (77 mg, 0.478 mmol) in DMF (2 mL) was added DIPEA (0.25 mL, 1.43 mmol) at 0 °C. The resulting reaction mixture was stirred at RT for 24 h and monitored by TLC and LC-MS. After the reaction was completed, the reaction mixture was cooled, diluted with water (5 mL), and extracted with ethyl acetate (2 × 30 mL). The separated organic layer was washed with water and brine, dried

over sodium sulfate, filtered, and concentrated under reduced pressure to afford the crude product. Which was purified by Grace using 12 g of silica (REVELERIS) eluted with 40–50% of ethyl acetate in pet-ether to get (93 mg, 0.275 mmol, 65%) 6-chloro-4-(3-isonicotinoylazetidin-1-yl)pyridazine-3(2*H*)-one **45** as a pale yellow solid. ^{1}H-NMR (400 MHz, DMSO-d_6): δ 12.51 (s, 1H), 8.84 (dd, $J = 4.8$ Hz, $J = 1.6$ Hz, 2H), 7.76 (dd, $J = 4.8$ Hz, $J = 1.6$ Hz, 2H), 6.01 (s, 1H), 4.61–4.30 (m, 5H); LC-MS (ES-API): $m/z = 291.1$ $(M + H)^+$, purity by LC-MS: 96.7%.

*5.2.4.37. Preparation of 4-(3-isonicotinoylazetidin-1-yl)-6-(pyridin-4-yl)pyridazin-3(2H)-one (**46**).* To a stirred solution of 6-chloro-4-(3-isonicotinoylazetidin-1-yl)pyridazin-3(2*H*)-one **45** (90 mg, 0.310 mmol) in 1,4-dioxane (5 mL) were added 2 N Na_2CO_3 (98 mg, 0.93 mmol, 3.0 equiv), pyridin-4-yl boronic acid (57 mg, 0.465 mmol, 1.5 equiv.) and degassed with argon for 5 minutes prior to the addition of Pd(dppf)$Cl_2 \cdot CH_2Cl_2$ (24 mg, 0.03 mmol, 0.1 equiv.) and stirred at 100 °C for 16 h. The reaction mixture was diluted with ice-cold water (20 mL) and extracted with EtOAc (2 × 30 mL). The combined organic layer was washed with brine (10 mL), dried over anhydrous Na_2SO_4, filtered, and concentrated under reduced pressure to afford crude compound, which, upon purification by flash chromatography (using Biotage, Claricep, 12 g silica cartridge, eluted with 5–10% of MeOH in CH_2Cl_2) to afford (51 mg, 0.153 mmol, 48%) 4-(3-isonicotinoylazetidin-1-yl)-6-(pyridin-4-yl)pyridazin-3(2*H*)-one **46** as a pale yellow solid. ^{1}H-NMR (400 MHz, DMSO-d_6): δ 12.80 (s, 1H), 8.63 (dd, $J = 4.4$ Hz, $J = 1.6$ Hz, 2H), 8.63 (dd, $J = 4.4$ Hz, $J = 1.6$ Hz, 2H), 7.82–7.78 (m, 4H), 6.60 (s, 1H), 4.61–4.40 (m, 5H); ^{13}C-NMR (400 MHz, DMSO-d_6): 197.8, 156.6, 150.9, 150.0, 145.2, 143.0, 140.5, 121.3, 119.9, 98.7, 37.4; IR: 1641.4 cm^{-1} (C═O stretching); LC-MS (ES-API): $m/z = 334.16$ $(M + H)^+$; purity by LC-MS: 94.8%; MR: 262–265 °C.

*5.2.4.38. Preparation of tert-butyl 3-(4-fluorobenzoyl) azetidine-1-carboxylate (**49**).*[21] To a stirred solution of 1-bromo-4-fluorobenzene **48** (398.436 mg, 2.277 mmol, 1 equiv.) in tetrahydrofuran (10 mL) was added *n*-butyl lithium (1.6 M hexanes 1.7 mL, 2.732 mmol, 1.2 equiv.) at −78 °C under nitrogen atmosphere and the reaction mixture was stirred at −78 °C for 1 h, before the addition of *tert*-butyl 3-(methoxy(methyl)carbamoyl)azetidine-1-carboxylate **47** (500 mg, 2.049 mmol, 0.9 equiv.). The reaction mixture was stirred at the same temperature for another 1 h. The reaction mixture was quenched with saturated NH_4Cl solution, and the aqueous layer was extracted with EtOAc (2 × 80 mL). The combined organic layer was washed with brine (50 mL), dried over anhydrous Na_2SO_4, filtered, and concentrated under reduced pressure to obtain crude compound, which upon purification by flash chromatography (BUCHI Claricep, 40 g silica cartridge, eluting with 20–30% EtOAc/pet-ether) to get (250 mg, 0.896 mmol, 43%) of *tert*-butyl 3-(4-fluorobenzoyl) azetidine-1-carboxylate **49** as a white solid.^{1}H-NMR (400 MHz, $CDCl_3$): δ 7.88–7.84 (m, 2H), 7.18–7.13 (m, 2H), 4.82 (s, 1H), 4.22–4.08 (m, 4H), 3.41 (m, 2H), 1.44 (s, 9H); LC-MS (ES-API): $m/z = 280.14$ $(M + H)^+$, purity by LC-MS: 92.8%.

*5.2.4.39. Preparation of azetidin-3-yl(4-fluorophenyl) methanon hydrogen chloride (**50**).* To a stirred solution of *tert*-butyl 3-(4-fluorobenzoyl)azetidine-1-carboxylate **49** (250 mg, 0.895 mmol, 1 equiv.) in 1,4-dioxane (10 mL) was added 4 M HCl in 1,4-dioxane at 0 °C and allowed the reaction to stir at RT for 2 h. The reaction mixture was concentrated under reduced pressure to remove excess HCl, and the residue was triturated with diethyl ether (20 mL), decanted, and the solid was dried to afford (120 mg, 0.43 mmol, 62%) of azetidin-3-yl(4-fluorophenyl)methanon hydrogen chloride **50** as a white solid. LC-MS (ES-API): $m/z = 280.14$ $(M + H)^+$, purity by LC-MS: 76.3%.

*5.2.4.40. Preparation of 6-chloro-4-(3-(4-fluorobenzoyl)azetidin-1-yl)pyridazin-3(2H)-one (**51**).* To a stirred solution of azetidin-3-yl(4-fluorophenyl)methanone hydrogen chloride **50** (120 mg, 0.558 mmol, 1.0 equiv.) in DMF (5 mL) were added 4-bromo-6-chloropyridazin-3(2*H*)-one **5** (120 mg, 0.558 mmol, 1.0 equiv.) and DIPEA (0.3 mL, 1.674 mmol, 3 equiv.) at 0 °C under nitrogen atmosphere and allowed the reaction mixture to stir at RT for 16 h.The reaction mixture was diluted with ice-cold water (10 mL) and extracted with ethyl acetate (EtOAc) (2 × 30 mL). The combined organic layer was washed with brine (10 mL), dried over anhydrous Na_2SO_4, filtered, and concentrated under reduced pressure to afford the crude product, which, upon purification by flash chromatography (using Biotage, Claricep, 12 g silica cartridge, eluted with 5–10% of MeOH in CH_2Cl_2) to afford (130 mg, 0.42 mmol, 76%) 6-chloro-4-(3-(4-fluorobenzoyl) azetidin-1-yl)pyridazin-3(2*H*)-one **51** as a pale yellow solid. LC-MS (ES-API): $m/z = 308.25$ $(M + H)^+$, purity by LC-MS: 81.9%.

*5.2.4.41. Preparation of 4-(3-(4-fluorobenzoyl)azetidin-1-yl)-6-(pyridin-4-yl)pyridazin-3(2H)-one (**52**).* To a stirred solution of 6-chloro-4-(3-(4-fluorobenzoyl)azetidin-1-yl)pyridazin-3(2*H*)-one **51** (130 mg, 0.422 mmol, 1.0 equiv.) in 1,4-dioxane (10 mL) were added 2 N Na_2CO_3 (134 mg, 1.266 mmol, 3.0 equiv), pyridin-4-yl boronic acid (67.4 mg, 0.548 mmol, 1.3 equiv.) and degassed with argon for 5 minutes prior to the addition of Pd(dppf)$Cl_2 \cdot CH_2Cl_2$ (34 mg, 0.042 mmol, 0.1 equiv.) and stirred at 100 °C for 16 h. The reaction mixture was diluted with ice-cold water (20 mL) and then extracted with EtOAc (2 × 30 mL). The combined organic layer was washed with brine (10 mL), dried over anhydrous Na_2SO_4, filtered, and concentrated under reduced pressure to afford crude compound, which, upon purification by flash chromatography (using Biotage, Claricep, 12 g silica cartridge, eluted with 5–10% of MeOH in CH_2Cl_2) to afford (16 mg, 0.045 mmol, 17%) 4-(3-(4-fluorobenzoyl)azetidin-1-yl)-6-(pyridin-4-yl)pyridazin-3(2*H*)-one **52** as an off-white solid. ^{1}H-NMR (400 MHz, DMSO-d_6): δ 12.78 (s, 1H), 8.63 (d, $J = 4.4$ Hz, 2H), 8.03–7.99 (m, 2H), 7.82 (d, $J = 6.0$ Hz, 2H), 7.40 (t, $J = 8.8$ Hz, 2H), 6.59 (s, 1H), 4.58–4.38 (m, 5H); ^{13}C-NMR (400 MHz, DMSO-d_6): 190.2, 166.2, 164.0, 156.6, 150.0, 145.2, 143.0, 131.3, 131.2, 120.2, 116.1, 115.9, 98.9, 37.0; IR: 1641.4 cm^{-1} (C═O stretching); LC-LC-MS (ES-API): $m/z = 351.32$ $(M + H)^+$. IR: 1658.7 cm^{-1} (C═O stretching); purity by HPLC: 94.6%; MR: 240–243 °C.

5.3. Cell lines

All cell lines utilized in this study were sourced from ATCC (Middlesex, UK) and DSMZ (Braunschweig, Germany). Cells were cultured at 37 °C in a humidified incubator with 5% CO_2 and atmospheric air. They were maintained in their

recommended growth medium, supplemented with 10% fetal calf serum (Gibco), 1× penicillin–streptomycin solution (Gibco) 2 mM glutamine (Gibco), 1 mM sodium bicarbonate (Gibco), 1 mM sodium pyruvate (Gibco), and 20 mM HEPES (Gibco). All cell lines were regularly authenticated and biweekly tested for mycoplasma using established laboratory protocols.[22,23]

5.4. Cytotoxicity assay

The cytotoxic effects of the compounds were evaluated using a standard 3-(4,5-dimethylthiazol-2-yl)-5-(3-carboxymethoxyphenyl)-2-(4-sulfophenyl)-2*H*-tetrazolium (MTS) assay, following 72 h of compound treatment in a panel of human cell lines. The assay was performed using the CellTiter 96® AQueous One Solution kit (Promega, USA) according to the validated protocol routinely used in our laboratory.[24]

The cell line panel consisted of cancer and non-cancer cell lines with varying ITK and BTK expression levels.[25] ITK or BTK null cancer cell lines included HCT116 (colorectal carcinoma, male), HCT116 p53−/− (colorectal carcinoma, p53 mutant, male), U2OS (osteosarcoma, female), and A549 (lung adenocarcinoma, male). Non-cancerous fibroblast lines included MRC-5 (lung, male, ITK/BTK null) and BJ (foreskin, male, ITK/BTK null). ITK-positive lines included Jurkat (T-cell leukemia, male) and CCRF-CEM (T-cell leukemia, female), whereas BTK-positive lines included RAMOS (B-cell lymphoma, male) and K562 (chronic myeloid leukemia, female).

All MTS cytotoxicity assays included DMSO-treated cells as negative controls. Ibrutinib has been profiled in parallel under identical screening conditions in our previous work and is routinely used as an internal benchmark for this assay.[14] Assays were performed on a robotic high-throughput screening platform (HighResBio, Boston, MA, USA) using a standardized protocol previously validated in our laboratory.[24] Dose–response curves were analyzed to determine IC_{50} values using Dotmatics software (San Diego, CA, USA). The results were archived in the MedChemBio database (https://www.medchembio.imtm.cz) and communicated to the medicinal chemists. The TI was calculated as the ratio of IC_{50} in fibroblast cells (BJ or MRC5) to that in Jurkat cells. For compounds that showed no measurable cytotoxicity in fibroblasts at concentrations up to 50 μM (IC_{50} > 50 μM), the TI was reported as 'n. d.'. In these cases, 50 μM was treated as the upper assay limit for TI estimation.

5.5. Molecular docking

Molecular docking was employed as a computational technique to predict the optimal binding mode of a ligand to a target protein. Scaffolds obtained through pharmacophore screening and synthesized compounds were subjected to molecular docking using AutoDock Vina. For this study, the 3D structure of the ITK protein, along with its known ligand (PDB: 3QGW),[13] was retrieved from the Protein Data Bank (PDB). Before docking, the protein structure was prepared to address elements not included in the X-ray crystallography refinement process. This preparation involved adding missing hydrogen atoms, optimizing hydrogen bonding, resolving atomic clashes, and making other necessary adjustments using UCSF Chimera.[26]

5.6. AutoDock Vina

Molecular docking was performed using AutoDock Vina to predict the binding modes of ligands with the target protein's three-dimensional structure. The program employs various computational docking techniques, including protein-ligand docking, blind docking, and site-specific docking. In addition to docking, AutoDock Vina, supported by AutoDock Tools, facilitated ligand and protein structural modifications. This approach enabled the evaluation of molecular assemblies of various sizes. The docking analysis provided key information, including binding energy, root mean square deviation (RMSD), and the number of hydrogen bonds (H-bonds) at position 44. The target protein's docking site was defined using a 21 × 21 × 21 Å grid box with the following coordinates: $X = 21$, $Y = -74$, and $Z = 24.2$ Å. Essential chemical interactions were observed within this grid box.[27]

5.7. *In vitro* biochemical kinase assay

Recombinant ITK and BTK enzyme activities were assessed using the ITK Kinase Assay Kit (BPS Biosciences, Cat. #78429) and the BTK Kinase Enzyme System (Promega, Cat. #V2941). Enzymes were diluted to 5 ng μL^{-1} in their respective assay buffers. For BTK, the buffer was supplemented with 50 μM DTT and 2 mM $MnCl_2$, as per the kit instructions.

Test compounds were evaluated across a 0–10 μM range by serial dilution in assay buffer containing 10% DMSO. Ibrutinib (100 nM) was included as a positive control. Compounds (1 μL per well) were dispensed into 384-well white opaque plates (Corning, Cat. #4513), and total reaction volume was maintained at 5 μL with <0.5% final DMSO.

ADP production was quantified using the ADP-Glo™ Kinase Assay (Promega, Cat. #V9101). Luminescence was recorded on a Tecan Infinite 200 PRO plate reader (integration time: 1000 ms; settle time: 200 ms). Activity was normalized to DMSO-only controls (100%) and background (0%), and IC_{50} values were calculated using a three-parameter logistic model in GraphPad Prism (GraphPad Software, Boston, MA, USA). The calculated IC_{50} values are presented as the mean ± standard error of the mean of 2–3 replicates.

5.8. Drug treatment and western blotting

Jurkat cells were seeded at a density of 0.5×10^6 cells per mL in 6-well cell culture plates and stimulated with 5 μg per mL PHA (phytohemagglutinin) in RPMI supplemented with 10% fetal calf serum for 15 minutes, as per established protocols,[28] followed by treatment with compound **9** at final concentrations of 10 μM, 2.25 μM, and 0.62 μM for 24 h. DMSO-treated cells served as vehicle controls (final DMSO concentration 0.1%). After treatment, cells were collected and washed in phosphate-buffered saline (PBS) and lysed in radioimmunoprecipitation assay (RIPA) buffer (Thermo Fisher, Cat. #89901) supplemented with protease and phosphatase inhibitors (Roche, Cat. #04693116001 and #04906837001). Cells were then sonicated at

4 °C (Qsonica Cup Horn sonicator, 25% amplitude, 1 min total, 5 s off/10 s on) and centrifuged at 13 000×*g* for 30 min. Protein concentrations in the supernatants were determined using the bicinchoninic acid assay (Thermo Fisher, Cat. #23223 and #23224).

Equal amounts of protein (30 μg) were separated by 10% sodium dodecyl sulfate–polyacrylamide gel electrophoresis and transferred onto nitrocellulose membranes (Bio-Rad, Cat. #170-4270) using the Trans-Blot Turbo system. Membranes were blocked with 5% bovine serum albumin (BSA) in Tris-buffered saline with Tween 20 (TBST), then incubated overnight or for 2 hours at 4 °C with the following primary antibodies: anti-interleukin-2-inducible T-cell kinase (ITK; 1 : 1000 dilution; Cell Signaling Technology, Catalog #2380S), anti-phospho-BTK/ITK (Tyr551/Tyr511), which detects the conserved activation-loop phosphorylation site shared by ITK and BTK (Tyr551/Tyr511; 5 μg mL^{-1}; Thermo Fisher, Catalog #14-9015-80), anti-p44/42 mitogen-activated protein kinase (MAPK; extracellular signal-regulated kinases 1 and 2, ERK1/2; 1 : 1000 dilution; Cell Signaling Technology, Catalog #9102S), anti-phospho-p44/42 MAPK (Thr202/Tyr204; 1 : 1000 dilution; Cell Signaling Technology, Catalog #4376S), and GAPDH (loading control) (Cell Signaling, Cat. #2118S). After washing, the membranes were incubated with Alexa Fluor 488-conjugated secondary antibodies (Invitrogen, Catalog #A21202 and #A11034) for 1–2 hours at room temperature in the dark. Blots were visualized using the ChemiDoc MP imaging system (Bio-Rad, California, United States). Band intensities were quantified using National Institutes of Health (NIH) ImageJ software and normalized to GAPDH as the loading control. Phosphorylated and total ITK and ERK band intensities were quantified as p-ITK/ITK and p-ERK/ERK ratios, respectively, normalized to GAPDH, and presented as normalized ratios.

6. Statistical analysis

Data were analyzed using GraphPad Prism software (GraphPad Software, Boston, Massachusetts, United States). Dose–response data were fitted using a three-parameter (or four-parameter, where appropriate) nonlinear logistic regression model to calculate IC_{50} values, reported as mean ± standard error of the mean from independent experiments (n = 2–3). Comparisons between two groups were assessed using unpaired two-tailed t-tests. Comparisons involving more than two groups were assessed using one-way analysis of variance (ANOVA) followed by post hoc multiple comparison tests. Statistical significance was set at $P < 0.05$. Error bars throughout represent SEM, and the number of independent replicates (n) is indicated in the figure legends.

Ethical statement

This study involved only established human cell lines and did not include experiments on human participants or animals. All procedures were conducted in accordance with institutional biosafety and laboratory practice guidelines.

Author contributions

Sudhakar Tangallapalli: methodology, investigation, formal analysis, visualization, writing – original draft. Rambabu Gundla: writing – review & editing, supervision, conceptualization, funding acquisition. Kalyani Paidikondala: formal analysis, data curation. Soňa Gurská: methodology, investigation. Naveen Kumar Rampeesa: investigation, formal analysis, data curation. Sreenivasa Reddy Anugu: resources, formal analysis, Petr Džubák: resources, funding acquisition. Marián Hajdúch: resources, funding acquisition, writing – review & editing. Viswanath Das: methodology, investigation, supervision, conceptualization, funding acquisition, writing – review & editing. Naresh Kumar Katari: conceptualization, and funding acquisition.

Conflicts of interest

Sudhakar Tangallapalli, Rambabu Gundla, Sreenivasa Anugu, and Viswanath Das are listed as inventors on a published patent application titled 'novel 3-oxo-2,3-dihydropyridazine derivatives as selective inhibitors of interleukin-2-inducible T-cell kinase (ITK), Indian Patent Application No. 202541061978 A. The remaining authors declare no competing interests.

Data availability

All data supporting the findings of this study are available in the manuscript or supplementary information (SI) files. Cytotoxicity data of compounds are stored in the IMTM Dotmatics database and MedChemBio Portal, and are available from the corresponding author (V. Das) upon reasonable request. Supplementary information is available. See DOI: https://doi.org/10.1039/d5ra06565h.

Acknowledgements

RG acknowledges GITAM for financial assistance and facility. ST, NKR, and SRA thank Aragen Lifesciences Pvt Ltd. Hyderabad, India, for providing computational resources for synthesizing and characterizing all the compounds by NMR, LC-MS, and FT-IR. All biological part of the study was supported in parts by the infrastructural projects (CZ-OPENSCREEN – LM2023052; EATRIS-CZ – LM2023053, BBMRI – LM2023033, and Czech-BioImaging – LM2023050, LM2018129), the projects National Institute for Cancer Research (Program EXCELES, ID Project No. LX22NPO5102, funded by the European Union – Next Generation EU), project SALVAGE (registration number: CZ.02.01.01/00/22_008/0004644, supported by OP JAK, with co-financing from the EU and the State Budget), all funded by the Ministry of Education, Youth and Sports of the Czech Republic, and the project TN02000109 (Personalized Medicine: From Translational Research into Biomedical Applications) co-financed with the state support of the Technology Agency of the Czech Republic as part of the National Centers of Competence Program. We would like to thank Ciencia Life Sciences for providing the docking studies.

References

1 U. Schmidt, N. Boucheron and F. Kiefer, *Trends Immunol.*, 2017, **38**(5), 342–355.
2 W. Huang, L. A. Solt and Y. Wang, *Front. Immunol.*, 2020, **11**, 1986.
3 A. J. Müller, O. Filipe-Santos, G. Eberl, T. Aebischer, G. F. Späth and P. Bousso, *Immunity*, 2012, **37**(1), 147–157.
4 J. Gomez-Rodriguez, J. A. Readinger, I. C. Viorritto and P. L. Schwartzberg, *Immunol. Rev.*, 2016, **231**(1), 45–56.
5 J. A. Readinger, K. L. Mueller, A. M. Venegas, R. Horai and P. L. Schwartzberg, *Nat. Rev. Immunol.*, 2008, **8**(10), 865–876.
6 J. Yayan, K. J. Franke, M. Berger, W. Windisch and K. Rasche, *Mol. Biol. Rep.*, 2024, **51**(1), 165.
7 Y. Liu, X. Wang and L. Deng, *Cancer Cell Int.*, 2019, **19**, 32.
8 K. Onidani, N. Miura, Y. Sugiura, Y. Abe, Y. Watabe, T. Kakuya, T. Mori, S. Yoshimoto, J. Adachi, T. Kiyoi, Y. Kabe, M. Suematsu, T. Tomonaga, T. Shibahara and K. Honda, *Cancers*, 2021, **13**(13), 3333.
9 E. M. Flefel, W. A. Tantawy, W. I. El-Sofany, M. El-Shahat, A. A. El-Sayed and D. N. Abd-Elshafy, *Molecules*, 2017, **22**(1), 148.
10 A. Malik, R. Mishra, R. Mazumder, A. Mazumder and P. S. Mishra, *Res. J. Pharm. Technol.*, 2021, **14**(6), 3423–3429.
11 M. Rimaz and H. Mousavi, *Turk. J. Chem.*, 2013, **37**, 252–261.
12 Z.-Q. Liu, Q. Zhang, Y.-L. Liu, X.-Q. Yu, R.-H. Chui, L.-L. Zhang, B. Zhao and L.-Y. Ma, *Bioorg. Med. Chem.*, 2024, **111**, 117847.
13 J. D. Charrier, A. Miller, D. P. Kay, G. Brenchley, H. C. Twin, P. N. Collier, S. Ramaya, S. B. Keily, S. J. Durrant, R. M. Knegtel, A. J. Tanner, K. Brown, A. P. Curnock and J. M. Jimenez, *J. Med. Chem.*, 2011, **54**, 2341–2353.
14 G. Muddasani, N. K. Rampeesa, S. Anugu, P. Muddasani, S. Gurská, P. Džubák, M. Hajdúch, V. Das and R. Gundla, *Bioorg. Med. Chem.*, 2025, **20**, 118116.
15 N. K. Rampeesa, *et al.*, *Bioorg. Chem.*, 2025, **157**, 108316.
16 L. Vargas, A. Hamasy, B. F. Nore and E. Smith, *Scand. J. Immunol.*, 2013, **78**, 130–139.
17 A. Shome, K. T. Jha and P. A. Chawla, *SynOpen*, 2023, **7**(4), 566–569.
18 J. W. B. Fyfe, N. J. Fazakerley and A. J. B. Watson, *Angew. Chem., Int. Ed.*, 2017, **56**(5), 1249–1253.
19 S. Noriko, E. Jun, N. Hiroshi, U. Megumi, S. Yusuke, I. Yusuke, A. Michiaki, H. Yuichi, K. Takeshi and Y. Koichi, WO2013147183, 2013.
20 D. M. Allwood, D. C. Blakemore, A. D. Brown and S. V. Ley, *J. Org. Chem.*, 2014, **79**(1), 328–338.
21 R. Duque, J. Lorena, Z. Brill, G. Fradera, X. Siliphaivanh, P. Su and J. Jing, WO2021252307, 2016.
22 R. Buriánová and J. Kotulová, *Laboratory Techniques in Cellular and Molecular Medicine*, Palacký University Olomouc, Olomouc, 1st edn, 2022, pp. 37–42.
23 J. Stránská, *Laboratory Techniques in Cellular and Molecular Medicine*, Palacký University Olomouc, Olomouc, 1st edn, 2022, pp. 29–36.
24 S. Gurská, *Laboratory Techniques in Cellular and Molecular Medicine*, Palacký University Olomouc, 1st edn, 2022, pp. 67–72.
25 C. P. Koraboina, V. C. Maddipati, N. Annadurai, S. Gurská, P. Džubák, M. Hajdúch, V. Das and R. Gundla, *ChemMedChem*, 2024, **19**(1), e202300511.
26 F. Pettersen, T. D. Goddard, C. C. Huang, S. Couch, D. M. Greenblatt, E. C. Meng and T. E. Ferrin, *J. Comput. Chem.*, 2004, **25**(13), 1605–1612.
27 O. Trott and A. J. Olson, *J. Comput. Chem.*, 2010, **31**, 455–461.
28 J. Ramchmilewitz, G. J. Riely, J. H. Huang, A. Chen and M. L. Tykocinski, *Blood*, 2001, **98**, 1656.